SOUTHERN GEOSCIENCE CONSULTANTS

Southern Geoscience Consultants Pty Ltd ACN 067 552 461
Level 1, 183 Great Eastern Highway, Belmont WA 6104 AUSTRALIA
PO Box 694, Belmont WA 6984 AUSTRALIA
T +61 (8) 6254 5000 F +61 (8) 6254 5099
E geophysics@sgc.com.au W www.sgc.com.au

MEMORANDUM

TO	Louis Hissink
FROM	Paul Mutton
DATE	10/6/2011
RE	Caranbirini VTEM Interpretation

Louis,

The interpretation of the Caranbirini VTEM survey is attached as Figure 1. Eleven targets have been identified for McArthur River Pb-Zn-Ag style mineralisation. The targeting features, processing products, interpretation methodology, and brief description of interpretation features are discussed below.

1 TARGET DESCRIPTION

The target for this survey is weakly conductive iron sulphides that may be associated with economic Lead-Zinc SEDEX sulphides. The exploration model is the McArthur River mine "HYC" orebody that is located 11.5km to the SE of the tenement. The HYC mineralisation model is shown in Appendix A (from the Xstrata website). A more complete description is given in Appendix B, (from Economic Geology of Australia and Papua New Guinea, 1. Metals). A summary of the geophysical signature of the HYC orebody is given in Appendix C (from the Exploration Geophysics journal.

Lead and Zinc sulphides are not conductive, however the associated pyritic shales and siltstones hosting the mineralisation assemblage conductive and the HYC orebody is described in literature as conductive. The airborne contours from a 20 year old airborne EM (Questem) survey over the HYC orebody is shown in Figure 2. It is clear that the conductor is the pyrite that extends beyond the orebody outline. It is interesting to note the size and scale of the anomaly.

The metal containing exhalative fluids containing is understood to have originated from vents along nearby faults (such as the Emu Fault) and settled in sediments in the adjacent basins. Close proximity to faults indicates higher prospectively. Other conductors that may exist in the area are carbonaceous and barren sulphidic sediments. They may form more extensive layers so discrete (1km x 3km) conductors are much more prospective than extensive (>5km long) conductors.

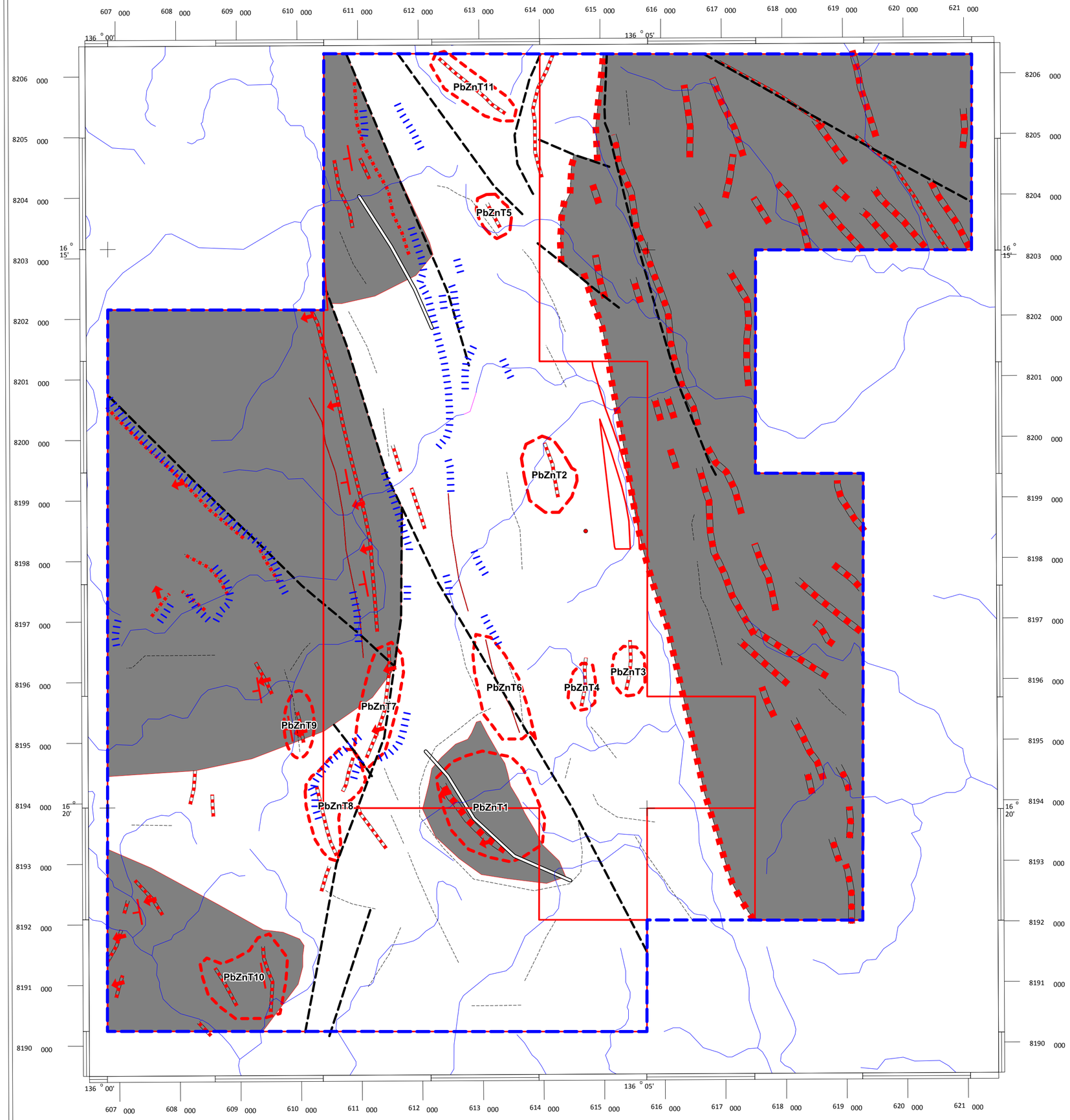

LEGEND - HEM INTERPRETATION

- HEM conductor axis - weak conductor
- HEM conductor axis - moderate conductor
- HEM conductor edge
- Anomaly Peak migration (to centre of conductor)
- Estimated conductor dip direction
- Extensive subhorizontal conductor (formational)
- Polarisation Anomaly Axis
- Magnetic anomaly trend
- Possible Fold Axis
- Possible Fault Location
- PbZnT2 Pb-Zn (McArthur River style) target & number
- Watercourse
- Mineralisation Occurence (250K sheet)
- 2010 VTEM Survey outline - 200m line spacing
- Brumby Resources Tenement outline

Note on targeting EM conductors for Lead Zinc sulphides

Zinc and Lead sulphides are non-conductive however they are frequenty associated with Iron sulphides that can be very conductive and the whole mineralisation assemblage is detectable with EM systems.

The McArthur River Mine is associated with iron sulphides and the mineralisation package is conductive.

N

0 2,500 5,000

meters

SCALE 1:50 000

DATUM: GDA94
GRID: MGA ZONE 53S

SOUTHERN GEOSCIENCE CONSULTANTS

BRUMBY RESOURCES LTD

CARANBIRINI PROJECT

2010 AIRBORNE EM (VTEM) INTERPRETATION

SCALE: 1:50 000	GEO: P. MUTTON
DATE: 10-06-2011	FIGURE 1

www.sgc.com.au

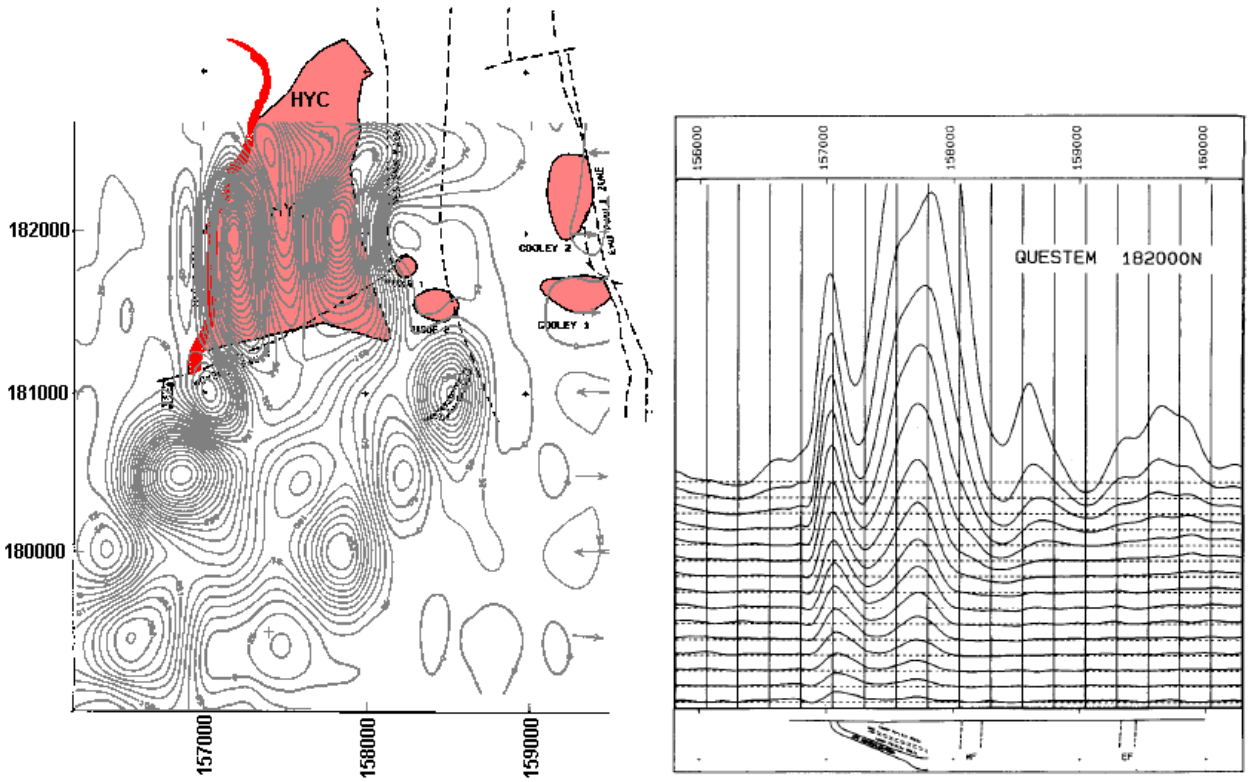

Figure 2 Plan view of Questem late time contours over the HTC mineralisation outline and (right) Questem profile along line 182000N showing a clear anomaly over the HYC mineralisation.

2 PROCESSING PRODUCTS

The processing of the 2010 VTEM data consisted of:

1. Gridding and imaging the Z and X component Coil data (linear and non-linear colour stretches)
2. Gridding and imaging the Z and X component B-field data (linear and non-linear colour stretches)
3. Processing of Conductivity Depth Inversion (CDI) sections using the EMFlow algorithm
4. Gridding and imaging of depth slices of the CDI's
5. Profiles of the located data and CDI sections
6. Flight Lines (Mapinfo format)

In addition to the VTEM data, other open file datasets were also reprocessed. These included:

1. Magnetics: Merging into the National data grid (400m line data) detailed 50m, 200m survey data. Processing and filtering to produce a set of TMI, RTP, RTP1VD, Tilt, 2VD, Analytic Signal, VIAS, and ASVI geotiffs. Also contours of TMI, RTP, and RTP1VD for 1:50K plotting.
2. Radiometrics: Merging into the National data grid (400m line data) detailed 50m, 200m survey data. Processing and filtering to produce a set of images of Total Count, Potassium, Thorium, Uranium, and ratio products
3. DTM. Imagine of Aster DEM (30m cells), and contours (for 1:50K plotting)
4. Geocover: Satellite RGB image (15m cells)
5. Gravity Surveys. Extracting the data from the ASGO database and imaging Bouguer gravity (plus 1VD, 1HD, tilt angle).
6. EM datasets: Gridding Geotem and Questem datasets and merging with the VTEM data 4 equal channel times (linear and non linear images).

3 INTERPRETATION PROCESS & FEATURES

Firstly all anomalies were picked from the Z and X profile data with their attributes such as conductivity, dip indicators, estimated source depth, source type. These were plotted and with the aid of the EM and magnetic images, features such as conductive (or chargeable) axis, dip indicators and fault locations were added.

The interpretation features used in the interpretation plan are:

Conductor Axis: This axis is aimed to be close to the up-dip expression of the conductive unit. Where dip indicators are visible (i.e. peak migration, anomaly asymmetry) they are located near the conductor axis. At Caranbirini where the conductors are very flat- lying it is sometimes difficult to determine the edge of the conductor.

Conductor Edge: This feature is at the edge of a horizontal or sub-horizontal unit. The Emu fault location is marked by the edge of the conductor as the formations to the east of the fault are weakly conductive and the boundary is quite distinct.

Anomaly Peak Migration and Dip direction: Interpreted from the profile data these indicators shows what direction the conductive unit extends from the conductor axis.

Extensive subhorizontal conductor: This is an extensive (more likely to be formational) conductive unit. The ground to the east of the Emu Fault is moderately conductive.

Polarisation Anomaly Axis: The causes of these are varied, not well understood, and are not considered to be targets. They are caused by shallow features, which may be related to faults, contacts, surficial clay layers or very shallow sulphidic/carbonaceous units.

Magnetic Anomaly trend: These are weak magnetic anomalies that are likely to indicate stratigraphic trends within sediments

Possible Fold Axis: From a combination of EM and magnetic data.

Possible Fault location: Interpreted from the terminations of magnetic and conductive units.

Pb-Zn target: Conductors located close to faults with dimensions similar to the target size.

4 TARGETS & RECOMMENDATIONS

Eleven targets have been outlined in Figure 1 and are listed in Table 1. No targets have been made to the West of the Emu Fault as the units are in a much younger group than the known zinc mineralisation.

The pyritic footprint of the HYC mineralisation is quite large. Surface reconnaissance of the target areas may reveal the source of some of the conductors and geochemical sampling may assist in prioritising drill targets.

Gravity and IP are additional techniques that have reportedly been successful in defining the limits of the HYC basin and may prove to be useful.

The EM targets have not been modelled and this is recommended prior to drill testing ensure the conductor is tested in an optimal position and to provide a better position.

Target ID	Priority	Scale	Description
PbZnT1	1	2 x 1.5km	moderately conductive discrete anomaly about a fold axis
PbZnT2	1	1 x 0.5km	weak conductor near Emu Fault in basin 500m from Zinc occurrence
PbZnT3	1	0.9 x 0.5km	Discrete, moderate conductor adjacent to Emu fault
PbZnT4	3	0.5 x 0.2km	weak, discrete conductor
PbZnT5	2	0.5 x 0.2km	small, discrete conductor near fault
PbZnT6	2	1.6 x 0.7km	Discrete conductor along possible fault.
PbZnT7	2	1.8 x 0.7km	Discrete conductor along possible fault.
PbZnT8	3	1.6 x 1km	very weak shallow conductors, possibly surficial
PbZnT9	2	0.6 x 0.2km	weak discrete conductor
PbZnT10	2	1.2 x 1.2km	weak-moderate (deep?) conductor
PbZnT11	3	1.4 x 0.3km	weak, surficial

Table 1 VTEM target summary

APPENDIX A – HYC orebody mineralisation style (from Xstrata Website)

McArthur River (HYC) Deposit Model

The McArthur River (HYC) zinc-lead deposit is one of the largest in the world. Current mineral resources (Xstrata Annual Report 2006) are 157 Mt @ 11.3% Zn, 4.9% Pb and 49 g/t Ag.

It is an example of a sediment hosted (SEDEX) zinc-lead deposit, which are known from around the world. Sedex deposits are widely distributed in Northern Australia in the Mount Isa – McArthur River region, eg. Mount Isa, Hilton, George Fisher, Lady Loretta, Dugald River, Century, and McArthur River.

Deposit features include:

- Fine-grained galena and sphalerite, with pyrite and pyrrhotite
- Good geophysical targets (eg. EM, IP, gravity, conductivity).
- Generally there is either a iron-manganese or a silicate alteration halo.
- Syn-sedimentary and replacement ore textures.
- Comprise 50% of the world's zinc and lead reserves, and 25% of world zinc and lead production.

McArthur River Basin rocks occur widely within the Reward EL 10316. The Barney Creek Formation and associated units is widespread.

A schematic east-west cross-section through the McArthur River (HYC) deposit is shown in Figure 1 below. It shows the HYC deposit occurring at or near the base of the HYC Pyritic Shale Member and comparison with the Myrtle prospect shows a close similarity. The proximity of faults (eg. Western, Emu Fault) is regarded as being important in the genesis of the HYC and associated (Ridge, Cooley) deposits. Similar faults have been interpreted at Myrtle.

Other prospects in the Reward EL, including Berjaya, Buffalo Lagoon, and Barney Creek Sub-basin, show similarities to the HYC deposit model also, although exploration is at an early stage.

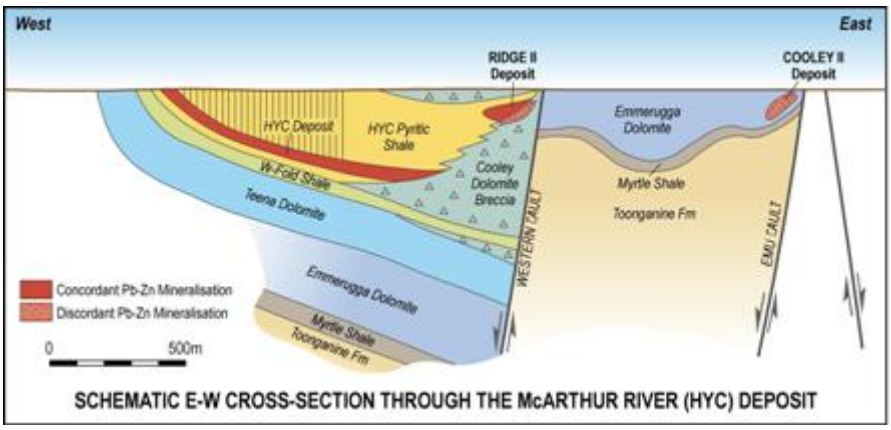

Figure 1: Schematic E-W Cross-Section through the McArthur River (HYC) Deposit (after Williams 1978)

A model for the deposition of McArthur River has been developed by Ireland et. al. (2004) and is shown in Figures 2 and 3 below. The source of metals (Zn and Pb ions) is from a fault system tapping these at depth in the Earth's crust. The metal ions are circulated into a shallow (~600-800m) marine basin with restricted circulation, and precipitate to form sulphide minerals (ZnS and PbS) at a depth below the Redox front (where free oxygen no longer exists).

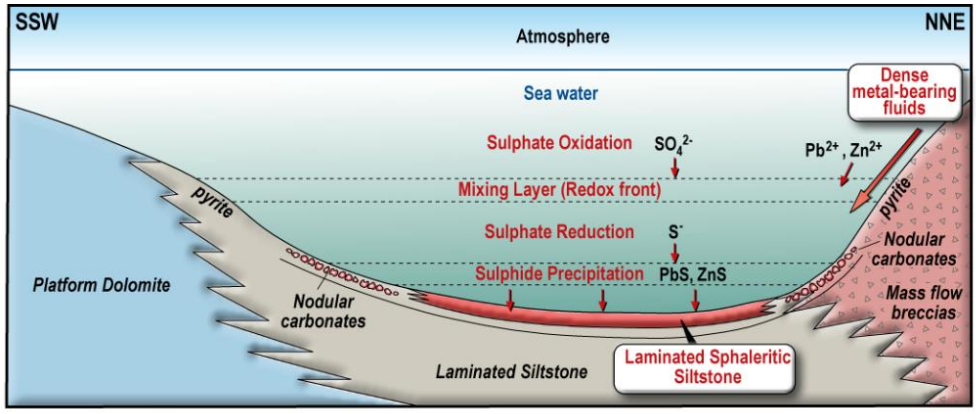

Figure 2: Cross Section of McArthur River deposit model showing the source of metal ions and the interpreted depth of sulphide precipitation (after Ireland et. al., 2004).

Of interest, in terms of exploration, is that the "fringe" zones to the highest grade mineralisation at the bottom of the basin is the development of "nodular carbonates" at shallower depths where some oxygen still exists in the form of SO_4^{2-} ions. This zone generally contains zinc mineralisation in the 5-7% grade range, and is very similar to what has been found at Myrtle so far. When viewed in plan (Figure 3) this nodular carbonate zone at McArthur River can be seen to surround the higher grade zone.

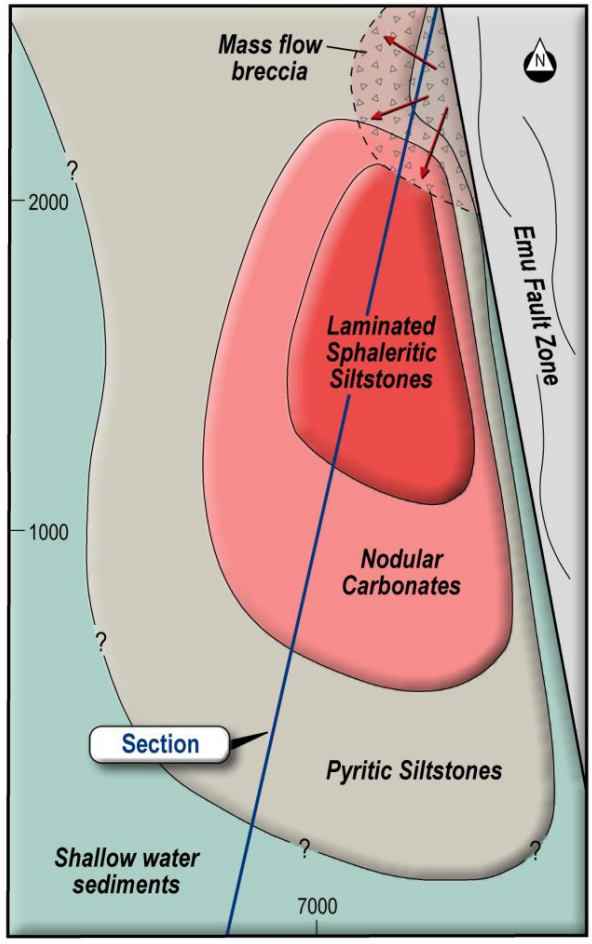

Figure 3: Plan of McArthur River deposit model showing the central high grade laminated siltstone surrounded by the medium grade nodular carbonate zone (after Ireland et. al., 2004).

APPENDIX B –Geology of HYC orebody

Murray, W.J. (1975) McArthur river H.Y.C Lead-Zinc and Related Deposits, N.T. *in* Knight, C.L (Ed) Economic Geology of Australia and Papua New Guinea, The Australasian Institute of Mining and Metallurgy,

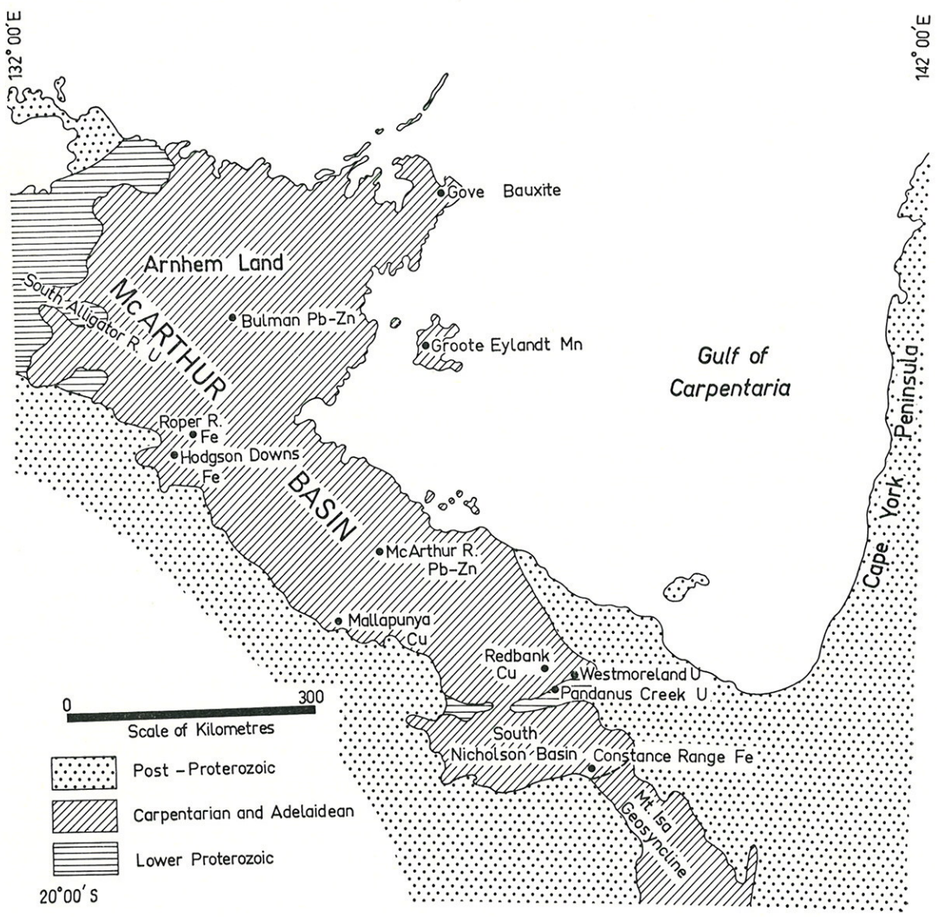

FIG. 1—McArthur and South Nicholson basins; based on Tectonic Map of Australia and New Guinea, 1971.

known as the *Eva* prospect, has been the only significant producer. At this mine, pitchblende and secondary uranium minerals are irregularly distributed in sheared acid to intermediate lavas and interbedded sandstones of ?Lower Proterozoic Cliffdale Volcanics immediately below the unconformably overlying Westmoreland Conglomerate, and very close to a small offshoot of the Nicholson Granite which intrudes the Cliffdale Volcanics but is unconformably overlain by the Westmoreland Conglomerate. Morgan (1965) records a production of 306 tonnes, averaging 8·37 per cent U_3O_8, from this mine.

Another group of small uranium prospects, of which the *Cobar 2* about 20 km north of Pandanus Creek is the most important, occur in the Peters Creek Volcanics, a predominantly basaltic sequence which unconformably overlies the Westmoreland Conglomerate. Individual ore shoots again are confined largely to shear zones and at Cobar 2 are associated with extensive hematitic replacements of the country rocks. Recorded production amounts to about 6 300 kg U_3O_8 in concentrates.

Minor copper tin and wolfram mineralization has also been recorded from the Cliffdale Volcanics and the Norris Granite within this general area. The mineralization is associated with quartz veins and greisen zones, at least some of which appear to have been controlled by major shear zones, such as the north-west trending Calvert Fault.

MINERALIZATION IN ADELAIDEAN ROCKS

In the Adelaidean rocks of the area, sedimentary iron ores are the only known mineral deposits of posssible economic importance. In the Roper River and Hodgson Downs areas, oolitic and pisolitic ironstones in the *Sherwin Ironstone Member* of the McMinn Formation have been extensively investigated by the Broken Hill Pty. Co. Ltd. (Canavan, 1965). In the Roper River area three separate beds of ironstone have been recorded, generally ranging in thickness from 2 to about 5 m with a maximum of about 12 m, and separated respectively by about 6 m and 15 m of sandstone and shale. Only one bed has been recognized in the Hodgson Downs area. The ironstone consists of oolites and pisolites, largely of hematite and goethite, from 0·2 to about 8 mm in diameter, in a matrix of siderite and minor chamosite and greenalite. Some of the oolites have silica grains as nuclei. Bladed hematite also occurs in the matrix, indicating some recrystallization and possibly small scale remobilization of iron in the rock. Dips of the beds are generally of the order of 5° to 10°. Ripple marks, mud cracks and cross-bedding are present, indicating shallow water conditions of deposition. Canavan (1965) has inferred in this general area 400 million tonnes with grades of 30 to 52 per cent iron, under overburden ratios of less than 2:1. However, high silica contents in most of this material makes it currently unattractive.

Similar oolitic ironstones occur within the Mullera Formation in the *Constance Range* area, about 250 km north-west of Mount Isa (Carter, Brooks & Walker, 1961; Harms, 1965). Hematite, siderite, chamosite and quartz are the major constituents of the unaltered ore, but replacement of siderite and chamosite by limonite and hematite has resulted commonly in enrichment of the near-surface material. All the iron-rich beds occur within a restricted stratigraphic interval, not more than 200 m thick, but individual beds within this sequence show considerable range in thickness and grade. Twelve separate deposits have been recorded within an area of about 40 by 60 km. The beds are broadly folded generally with dips of less than 30°, and have also undergone minor faulting. Deposition under shallow water conditions is again indicated by cross-bedding, ripple marks and mud cracks in the rocks associated with the ironstones. The deposits have been extensively investigated by the Broken Hill Pty. Co. Ltd., and Harms (1965) estimated reserves in the largest deposit at 257 million tonnes averaging 51.5 per cent iron, which could be upgraded to 59.9 per cent by calcination. In addition, reserves of oxidised ore at three deposits were estimated to total 40 million tonnes, averaging 57 per cent iron.

REFERENCES

Canavan, F., 1965. Roper Bar iron ore deposits in *Geology of Australian Ore Deposits,* (Ed. J. McAndrew) pp 212-215 (Eighth Commonwealth Mining and Metallurgical Congress: Melbourne).

Carter, E. K., Brooks, J. H., and Walker, K. R., 1961. The Precambrian mineral belt of north-western Queensland, *Bull. Bur. Miner. Resour. Geol. Geophys. Aust.*, 51.

Harms, J. E., 1965. Iron ore deposits of Constance Range in *Geology of Australian Ore Deposits* (Ed. J. McAndrew) pp. 264-269 (Eighth Commonwealth Mining and Metallurgical Congress: Melbourne).

Morgan, B. D., 1965. Uranium ore deposits of Pandanus Creek, Ibid. pp. 210-211.

Patterson, G. W., 1965. Lead-zinc ore deposits of Bulman, Ibid. pp. 194-196.

McARTHUR RIVER H.Y.C. LEAD-ZINC AND RELATED DEPOSITS, N.T.

by W. J. MURRAY[1]

SITUATION, DIMENSIONS, RESERVES

The H.Y.C. deposit is situated at lat. 16°26′S., long. 136°6′E. in the McArthur River District of the Northern Territory of Australia. It is a relatively shallow dipping stratiform orebody, of average thickness 50 m, in Middle Proterozoic shales. In plan view it has a maximum width of 1·05 km and a length of 1·65 km and it contains ore reserves in the order of 200 000 000 tonnes of some 10 per cent zinc and 4 per cent lead. The associated sediments are effectively unmetamorphosed. They have never been subjected to any substantial load or tectonic stress, and the typical structural pattern for the district is open

1 Regional Manager—Eastern Australia, Carpentaria Exploration Company Pty. Ltd.

basin and domal folding, disrupted only by simple normal faulting.

DISCOVERY

The deposit was originally located in 1955 by an inquisitive field assistant while engaged in soil geochemical sampling of a key section line within a 60 km by 60 km target area selected to search for Mount Isa type lead/zinc mineralization on the basis of regional geology and syngenetic thinking. While traversing across the black soil flood plains on the McArthur River he noted an isolated small jasper outcrop nearby and examination showed it to contain a considerable volume of white acicular crystals. Specimens were collected and later identified by geological staff as hemimorphite, but other larger discoveries made in the district the same year claimed priority for investigation. It was not until 1959 the first diamond core holes tested under the outcrop. Ironically, the jasper proved to be the surface expression of an otherwise barren breccia bed but the first hole penetrated the top of the zinc and lead bearing pyritic shales of the H.Y.C. orebody which lay some 20 m stratigraphically below.

Development of this major deposit has been hampered by several factors, the most serious of which are the formidable metallurgical difficulties occasioned by the extreme fine grained nature of the ore. Pending solution of these problems, testing of the deposit has been limited to that amount of drilling required to establish reserves. The surface is blanketed by deep alluvium, so it can be appreciated that many specific geological features of the deposit and its environs are still not clearly defined.

While drilling to establish the limits of the H.Y.C. deposits, a thick dolomitic reefal facies was found interfingering with the ore bearing shales. Scattered occurrences of weak mineralization were encountered in this dolomite and it was selected for later detailed examination as part of a continuing district exploration programme. Geophysical testing suggested the possible presence of sulphide accumulations, and increasing geological knowledge of the sub-soil geology, derived from rotary and diamond core drilling, has enabled several prospective small orebodies to be outlined.

REGIONAL GEOLOGICAL SETTING

The ore deposits occur on the eastern edge of a broad (+100 km) meridional rift valley which developed during the deposition of the McArthur Group sediments of the Middle Proterozoic Carpentarian System (Fig. 1). Subsidence of the rift floor allowed the accumulation of over 5 000 m of relatively shallow water carbonate muds, silts and arenites. Only the eastern edge is now exposed and today it is delineated by the Emu Fault System. This has a geologic history of movement during at least the Middle and Late Proterozoic, Cambrian and Cretaceous times, suggesting close relationship to a major basement lineament. The floor of the rift is visualized as gently sloping to flat, broken only by a meridional trending median ridge caused by occasional uplift along another probable major basement lineament which today is represented by the Tawallah Fault (Fig. 1).

Table 1 illustrates the stratigraphy of the lower units of the McArthur Group in the area between the Tawallah and Emu Faults (Fig. 2). Known mineralization consists of minor accumulations of disseminated sulphides in the Emmerugga and Teena Dolomites, and major deposits in both the H.Y.C. Pyritic Shale and Cooley Dolomite Members of the Barney Creek Formation. Several significant gross features relating to regional environment and sedimentary conditions should be noted.

1. All units thin as they approach the eastern platform and, to a lesser extent, the median uplift area. During deposition of the Teena Dolomite, this median area was occasionally

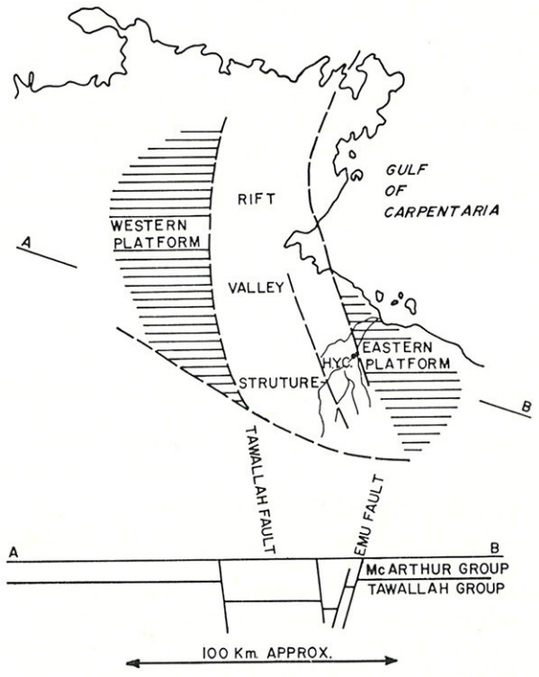

FIG. 1—Depositional environment of the McArthur Group.

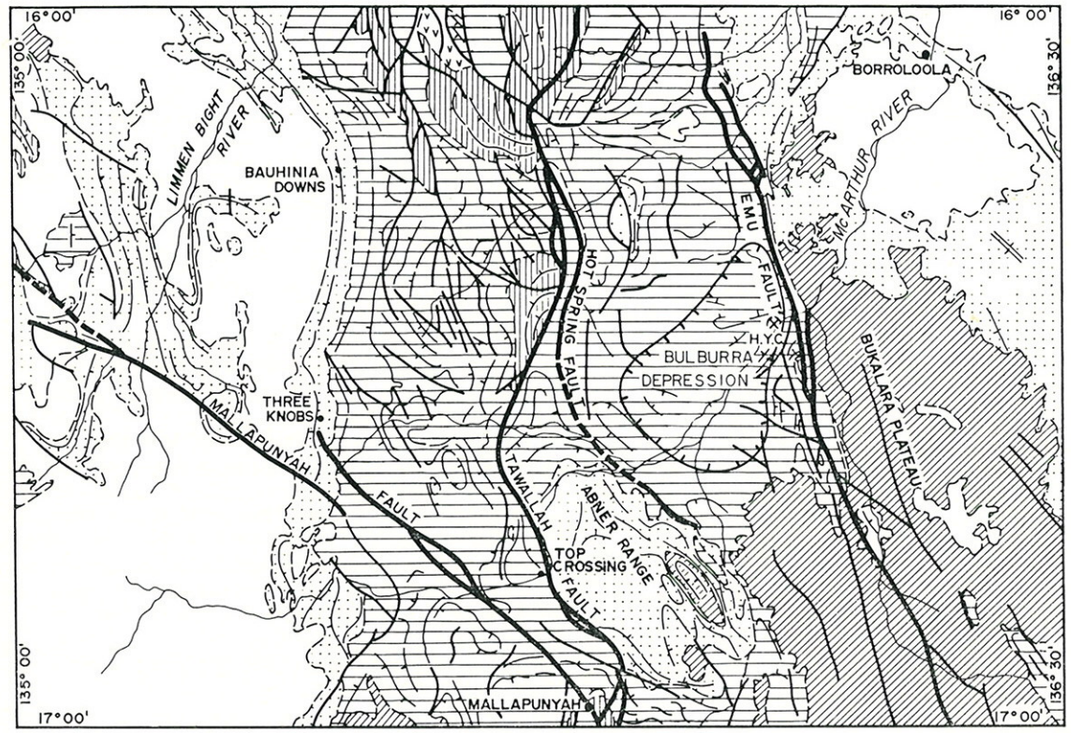

FIG. 2—Regional geology of the McArthur district. (Adapted from J. Smith 1964.)

elevated above sea level, restricting full development of the Barney Creek Formation to the eastern side of the trough and accounting for erosional unconformities higher in the sequence.

2. There is a variable tuff content in most sediments above the Tooganinie Formation. Tuff contribution appears to have reached a maximum during deposition of the W-Fold Shale Member at a period of time just prior to formation of the major syngenetic base metal deposits.

3. With the exception of the deep water reducing environment exhibited by the H.Y.C. Pyritic Shale Member, the McArthur Group sediments generally indicate shallow water deposition, varying in type from sub-aerial to shallow sub-tidal (Cotton, 1965; Munt, 1966; Shaw, 1967; Brown, 1969). This is demonstrated by the widespread occurrence of algal stromatolites and ooliths in carbonate units, and the occasional cross bedding and wave ripple marks that are found in silt and arenite sequences. Casts and molds of halite crystals in silty sections of some units indicate a saline water composition, and the considerable sulphide content of the H.Y.C. Pyritic Shale Member suggests a high sulphate availability.

LOCAL GEOLOGICAL SETTING

Throughout most of the McArthur exposures the Barney Creek Formation is represented by the shallow water dolomitic sediments of the Teena Member. However, during the late stages

TABLE 1

Stratigraphic column, Umbolooga Sub-Group of McArthur Group

(after B.M.R.—C.E.C., 1972)

FORMATION	MEMBER	GENERALIZED LITHOLOGY
REWARD DOLOMITE		Dolomite with characteristic chert pellets, dolomitic sandstone and chert, breccias, tuffs, local stromatolitic dolomite
	H.Y.C. Pyritic Shale	Bituminous and tuffaceous pyritic shale and dolomitic shale; tuff; local graded dolomitic arenites, dolomitic breccia; bedded base metal sulphides
BARNEY CREEK	Cooley Dolomite	Massive and brecciated dolomite, stromatolitic dolomite, minor sandstone and mudstone
	W-Fold Shale	Green tuff and red and brown tuffaceous dolomitic mudstone, dolomitic tuff, bituminous dolomite shale
TEENA DOLOMITE	Coxco Dolomite	Well laminated to thick bedded dolomite and rare dolomitic silt; occasional stromatolites
	Unnamed	As for above, with more silt sand and tuff content
EMMERUGGA DOLOMITE	Mitchell Yard Dolomite	Thick bedded clean dololutite with small irregular patches of dolomite spar; some tuffaceous silt and tuff beds
	Mara Dolomite	Cherty dololutite with stromatolites and algal lamination; minor dolomitic and tuffaceous mudstone and dolarenites
TOOGANINIE		Dolomite with some stromatolites and chert bands; some dolomitic shale silts sandstones, halite casts
	Myrtle Shale	Green and brown dolomitic shales; some sandstones
	Leila Sandstone	Dolomitic and quartz sandstone
TATOOLA SANDSTONE		Brown silts grading upwards to fine then coarse quartz sandstone with ripple marks
AMELIA DOLOMITE		Medium bedded dolomite, algal chert beds and mats; some siderite beds
MALLAPUNYAH		Purple silty dolomite; minor green micaceous shale and grey cherty silts

of deposition of this unit, local subsidence occurred over a 400 km² area, bounded by the active median ridge on the west and the eastern shelf line on the east. Here waters eventually reached sufficient depth to allow development of a bituminous pyritic shale environment. This particular area is now defined as the Bulburra Depression and the shale unit is the H.Y.C. Pyritic Shale Member. (It should be noted that the Bulburra Depression as illustrated by Cotton (1965) is regarded as the central tectonically folded portion of a more extensive area of basinal subsidence.) Along the eastern shelf line the pyritic shale unit is bordered in places by the Cooley Dolomite Member—a massive dolomitic unit displaying variously off-shore, lagoonal and reefal characteristics, where carbonate deposition and algal reef building kept pace with basinal subsidence.

Rate of subsidence on the floor of the Bulburra Depression was uneven, and on the eastern side this irregular downwarp allowed the development of several sub-basins in which greater than normal thicknesses of the H.Y.C. Pyritic Shale Member were deposited. Associated with these sub-basins are bedded base metal deposits. Those in the H.Y.C. sub-basin are by far the most significant economically, but the W-Fold sub-basin some 8 km to the west, and the Mitchell Yard sub-basin some 6 km to the south-west, contain mineralization of geological interest.

Though broad correlation is possible between the sub-basins, they probably reached the depths required for the development of a black shale-pyritic environment at different times. As a result, the base of significant pyritic shale content in the stratigraphic column cannot necessarily be taken to represent a time equivalent, and there is difficulty in establishing whether the syngenetic mineralization of the H.Y.C. sub-basin is precisely contemporaneous with other occurrences.

A considerable amount of purely stratigraphic drilling supplemented extensive regional mapping and it is clear from this that differing water depths and rates of subsidence have given rise to variations in the lateral lithofacies of units of the Barney Creek Formation. For example,

the carbonate sections of the Teena Member assume a thinner laminated character in deep sections as opposed to their more massive equivalents in the shallower environments. The W-Fold Shale Member is characterized in sub-basins by well bedded dark grey and green dolomitic sediments containing abundant fine volcanic shard material; the shallow water equivalent typically is a poorly bedded dolomite, often buff or pale green, lacking shards, but characterized by an abnormally high illite and potassium content. Adjacent to the eastern platform, both shallow and deeper types contain interbeds of carbonate sediment with a strong red coloration due to the presence of iron oxides of terrestrial origin.

The H.Y.C. Pyritic Shale Member, outside of the sub-basins, is usually a thin-bedded sequence of dark dolomitic, weakly pyritic and bituminous shales, devoid of base metal accumulations. It thins rapidly toward the edges of the Bulburra Depression, where the shales become progressively more dolomitic and less pyritic and bituminous. The Cooley Dolomite Member, as it is known to date, displays little stratigraphic variation other than facies changes. There are, however, considerable differences in algal content from section to section and there is a tendency for arenites and other off-shore sediments to become more plentiful toward the east.

THE H.Y.C. OREBODY

Geology

The H.Y.C. orebody occupies the floor of the relatively narrow H.Y.C. sub-basin and the generalized and informal stratigraphic column for this sub-basin is illustrated in Fig. 3 and in the idealized section Fig. 4. The orebody is separated from the greenish "Basal Tuff" unit by the "Lower Dolomitic Shales" which consist mainly of grey to black, well bedded, dolomitic shales. Throughout this unit are numerous thin uneven carbonate beds which impart a characteristic streaky appearance to drill core. Weakly developed pyritic shales and green tuff beds are relatively common within it. Tuff beds occur also in the overlying "Lower Pyritic Shales" and, along with tuffaceous shales, in limited numbers within the mineralized beds. Here they lack any characteristic coloration and a cherty appearance is the only indication of a high tuff content. To a large extent they resemble the "Tuff Marker Beds" of the mineralized Urquhart Shales of the Mount Isa district.

The "Pyritic Shale" units are characterized by the presence of bedded microspherical pyrite in quantities ranging from 3 to 30 per cent iron. They contain a minor but variable content of bituminous and tuffaceous material, and are divided into Upper and Lower sections by the less pyritic "Bituminous Shale" unit. All these shale units carry interbeds of dolomitic shales and silts and the latter often exhibit graded bedding on both microscopic and macroscopic scale. Sedimentary dolomitic breccias of turbidity origin interrupt the sequence and form a significant component of the "Lower Pyritic Shales", including the mineralized sections. These turbidity breccias were derived from the Cooley Member during time of orebody deposition, and higher in the sequence, similar sedimentation could have been derived from a now-eroded western reefal facies. Slumps and slump breccias are associated with the dolomitic sediments and turbidites on fore-reef slopes.

Mineralization

This has been described recently in detail (Croxford, 1967; Croxford and Jephcott, 1972). In brief, the sulphide ore minerals are associated with beds of dark bituminous, tuffaceous, and pyritic shales carrying varying but usually minor content of barren dolomitic shales, silts and thin breccia beds. They consist principally of pyrite galena and sphalerite, and marcasite arsenopyrite and chalcopyrite are minor accessories. Silver is associated with the galena in solid solution.

Pyrite occurs mainly as 1-15 micron spherical to isometric crystals. It forms delicately layered to massive bands, concordant with the shale bedding. Some coarse aggregate regrowths of this pyrite occur and these also trend parallel to shale bedding. Sphalerite occurs as monomineralic layers ranging from a few microns up to 1 mm in thickness, and as fine granular disseminations and elongate bodies up to 0·2 mm in diameter distributed discontinuously along bedding. Galena occurs as thin monomineralic layers up to 0·05 mm in thickness, or as sub-parallel discontinuous streaks within the sphalerite beds, and also as fine disseminations associated with sphalerite in the black shales. The fine sphalerite and galena layers invariably include the microspherical pyrite. Chalcopyrite is present in minor quantities as minute spindle shaped bodies within the layered sphalerite.

In hand specimen the ore is unspectacular. Low to medium grade lead and even high grade zinc mineralization often appears little different from barren pyritic shales. A dull grey appearance and excessive weight are the main indications of high grade lead bearing sections. Ore is never massive; it is finely bedded and the colour differences of alternating bituminous, pyritic, dolomitic, and rich ore beds helps to emphasize this. The orebody does contain a small proportion of

macroscopic sulphide minerals. These are found mainly in fractures, or more rarely as small discrete particles in micro-breccias or in dolarenite beds. In fractures they occur either as fine "paint" on faces or as crystalline fillings. Such fillings consist in order of relative abundance, of various combinations of carbonates pyrite sphalerite galena and chalcopyrite.

Features of the ore bearing sequence

The ore bearing sequence can be divided broadly into seven mineralized shale beds separated by six lower grade more dolomitic beds. This feature with respective average grades is illustrated diagrammatically in Fig. 3. The well mineralized beds are named Numbers 2 to 8 orebodies respectively up the section. The intervals between the orebodies are not specifically named but current usage tends towards naming them the 2/3 Beds, the 3/4 Beds, etc. These inter-ore beds are more variable in character than the mineralized beds.

Characteristics of the inter-ore beds

The 2/3 Beds resemble the "Lower Dolomitic Shales" and consist of pyritic and dolomitic shales and poorly bedded streaky or fragmented white dolomite. There is a general absence of any form of coarse grading. The 3/4 Beds are predominantly a sequence of graded dolomitic silts and minor shale. The other inter-ore beds are wedge-shaped and may range in thickness from in excess of 15 m on the eastern side of the sub-basin adjacent to the Cooley Dolomite Member, to some 20-30 cm on the western side. These inter-ore beds are composite in character and represent products of slump, slide and turbidity deposition of materials derived from the reef and back reef facies, and all types are usually represented within an individual inter-ore bed.

Slump breccias are dominant in the thicker northern and eastern sections of these inter-ore beds, and have been derived from material originally deposited on the fore-reef slope. Breccia fragments are usually angular blocks of siliceous dolomites, often quite large, set in a matrix of dolomitic or pyritic muds in which contortion of original bedding is discernible in places. The fragments often exhibit a rough grading in size suggesting sufficient hydroplasticity to allow sinking of the larger blocks. Any contained mineralization is associated only with those sections with a pyritic shale matrix.

Turbidite breccias assume relative importance within the central sections of the H.Y.C. deposit and they have a wider and more even areal distribution than slump breccias. They exhibit better grading of fragment sizes from bottom to top and are capped by successions of graded silts. Breccia fragments are exotic and consist mainly of angular to sub-angular siliceous grey brown and green dolomites, algal dolomites, and silts similar to those of the Cooley Dolomite Member. The matrix material is generally a dolomitic silt with a little disseminated fine grained pyrite. The thicker beds can contain basal fragments up to 30 cm across and where such sequences have been dumped upon the hydroplastic shales, the latter appears to have flowed upwards between the breccia fragments for appreciable distances.

In addition to slump and turbidite breccias the inter-ore beds contain thin dolomites, dolomitic silts and shales. Within the central and northern sections of the deposit these represent relatively quiet periods between deposition of the several breccia and graded beds that may make up one inter-ore interval. To the south and away from the Cooley Member the thinning turbidity breccias contain progressively smaller sized fragments, and towards the outer edge of the deposits they have become thin graded dolomitic silts and dolomites representing settling of the finer products of the slump and turbidity flows.

Characteristics of mineralized beds

The mineralized beds exhibit many features of penecontemporaneous deformation. They are commonly slumped and distorted at the base of major breccia beds and small scale load casts and slump structures, along with blind faulting and boudinage, are common throughout the ore sequence. In places there are small scale scour structures in ore beds at contacts with overlying turbidities, and submarine erosional surfaces or slump glide planes are probable explanations for suspected minor unconformities in ore beds. In two known cases several metres of the lower section of the ore bearing sequence are missing from drill intersections. This could be due to faulting, but a substantial slip of unconsolidated sediments is a more feasible explanation.

Slumping of ore beds on a larger scale is particularly evident in drill holes adjacent to the Cooley Dolomite Member, and is attributable to sliding down the fore-reef slope after sudden loading or disturbance.

Orebodies and metal ratios

The lead and zinc grades and ore thicknesses have been contoured for each individual orebody. Such contouring highlights the following generalizations.

1. No obvious relationships exist between thickness and grades of intersections. The out-

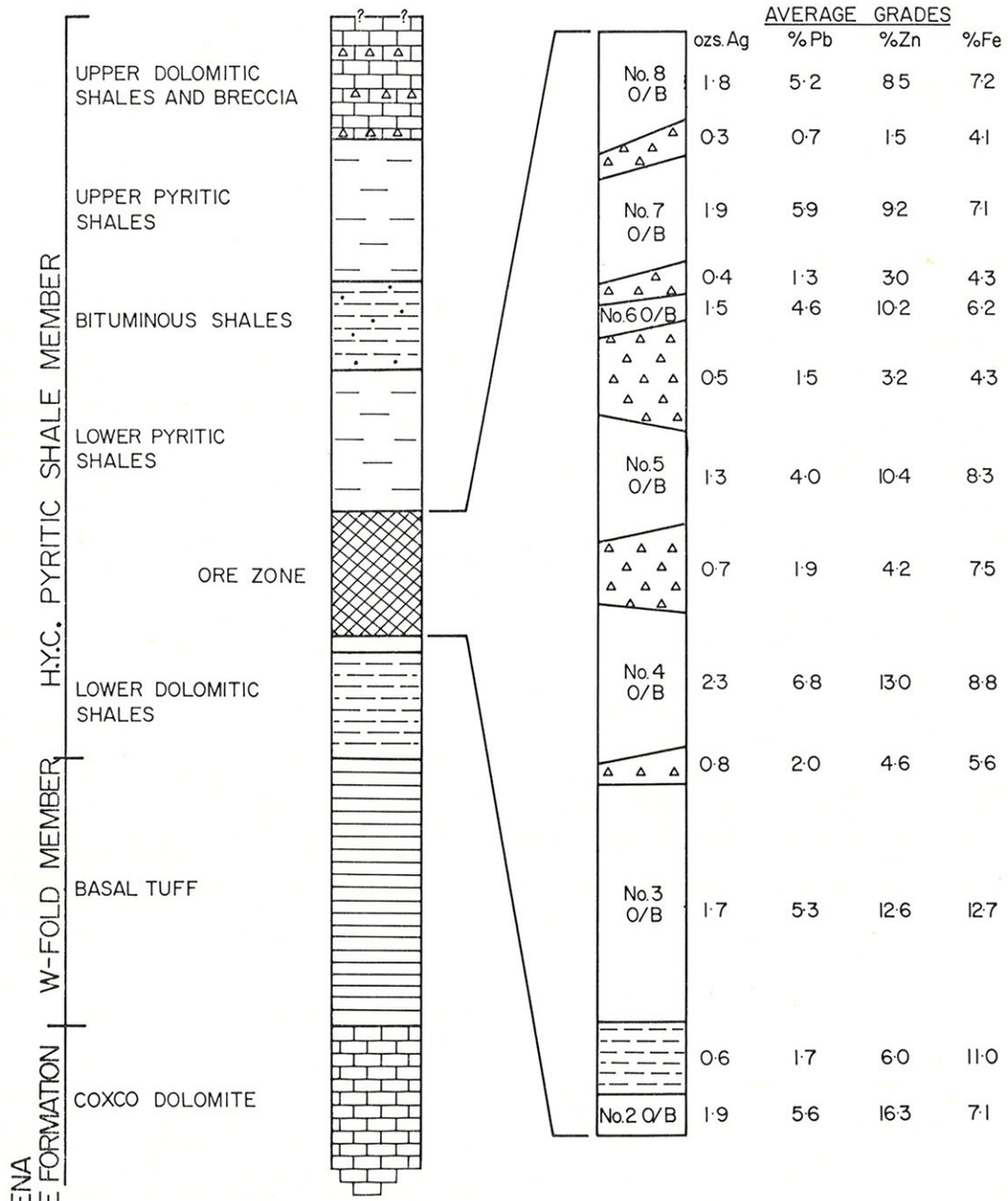

FIG. 3—Informal stratigraphic column for the H.Y.C. Sub-Basin showing orebody and inter-ore horizon grades.

ward decrease in ore grades is generally accompanied by an increase in the volume of dolomitic silts and a consequent increase in intersection thickness. The total thickness of the pyritic shale sections tends to remain relatively constant however, and within these pyrite content remains strong to the limits of drilling.

2. Lead grades drop off sharply as the outer margins of an orebody are approached but zinc values carry outward for greater distances and fall off only gradually. Peripheral ore consequently has higher zinc:lead ratios and this fact aids in the recognition of the source of slumped material in the fore-reef zone.
3. The higher grade portions of the lower orebodies are centrally placed, but in successive upper orebodies there is a general contraction in orebody size and the richer zone shifts towards the Cooley Dolomite Member.

Apart from the peripheral areas there is little lateral variation in lead:zinc:iron ratios within any individual orebody. Some of these are quite diagnostic and are of considerable assistance in initial gross correlation from drill hole to drill hole. There is a distinct vertical variation in metal contents and in ratios from orebody to orebody (Fig. 3). Zinc is the dominant sulphide metal of the H.Y.C. deposit and it clearly exhibits a gradual fall in values up the section. Lead values are more variable but actual Zn-Pb ratios suggest the presence of a repetitive pattern. A somewhat similar pattern exists in the Black Rock orebodies at Mount Isa and the figures are set out in Table 2 for comparison.

Silver values correlate closely with lead and consequently vary from orebody to orebody according to lead content.

TABLE 2

Zinc:lead ratios at H.Y.C. and Mount Isa

H.Y.C. Deposit		Mount Isa Black Rock	
Orebody	*Zn:Pb Ratio*	*Orebody*	*Pb:Zn Ratio*
8	1·63	6	1·80
	.....*		.....
		7	1·06
7	1·56	8	1·78
6	2·22	9	2·32
5	2·60	10	2·94
	.....		.....
4	1·91	11	1·20
3	2·38	11/30	1·29
2	2·91	11/66	1·61

*.....= pattern discontinuity

Copper exhibits the same bedded characteristics as the other metals. Values for individual orebodies vary over a wide range. The lower orebodies carry significant amounts of chalcopyrite, grades of individual selected beds being in excess of 0·5 per cent copper. Values for the upper orebodies are so low however that meaningful correlations cannot be drawn. Although chalcopyrite is almost exclusively associated with sphalerite, the zinc:copper metal ratio, either in bulk orebody assays or individual assay splits, is not particularly consistent.

The inter-ore intervals exhibit different metal ratio characteristics to those of the orebodies. Of these the 2/3 Beds must be considered apart as they represent normal shale sedimentation within the basin; they resemble the fringes of orebodies both in metal ratios and lithology. The other inter-ore intervals represent bulk dumping of sediments into the basin interrupting what otherwise would have been a continuous mineralized sediment sequence. Little significance can be attached to their individual metal ratios as they derive appreciable metal content from at least three sources.

1. Slump breccias have derived incorporated material from low grade peripheral type mineralization deposited on fore-reef slopes.
2. Pyritic shale material derived from the underlying orebeds is probably the most important source in the case of the thick turbidite breccias; values in this case can be expected to bear a relationship to those of the immediately underlying beds.
3. The presence of scour surfaces at the base of thin breccia beds suggests that turbidity currents could have often eroded the soft mineralized bottom sediments; such disturbed material would have settled in the breccia beds and accompanying graded silts.

BEDDED MINERALIZATION IN THE OTHER SUB-BASINS

Drilling of the other known sub-basins is limited because they have given little promise of immediate economic mineralization. The same stratigraphic divisions as in the H.Y.C. sub-basin can be observed in them, but boundaries are far more diffuse. The thick dolomitic sequences and graded breccias are absent, their place being taken by minor dolomitic silts and rare arenite bands. Probably these sub-basins were shallower and not flanked by reefal structures. There is also a tendency for pyritic shale beds to be a little coarser in appearance due to a greater degree of aggregation of the microspherical pyrite.

The W-Fold sub-basin is the only one to contain significant and potentially economic mineralization. Two deep diamond holes, over 1 500 m apart, have been drilled into it. Both were collared in Reward Dolomites, and both penetrated some 200 m of pyritic shales and 70 m of the "Basal Tuff" unit. One hole intersected 30 m of a little better than 3 per cent zinc including 2 m of 9 per cent zinc near the base, about 27 m above the "Basal Tuff" unit. The second hole intersected some 40 m of 2·2 per cent zinc including a basal 3 m of 9·5 per cent zinc, about 22 m above the "Basal Tuff".

Bedded microspherical pyrite becomes prominent only above the higher grade zinc bearing beds, which tend in appearance to resemble the streaky "Lower Dolomitic Shales" or the 2/3 Beds of the H.Y.C. orebody. Only a small proportion of the sphalerite in the richer zinc bearing section occurs in the same fine grained habit as that of the H.Y.C. deposit. Instead it is found as pale straw-yellow beds (up to 0·5 mm thick) interbedded with grey dolomitic shales. A few beds of similar thicknesses comprised of coarse grained red-brown sphalerite with subordinate galena crystals occur in the same sequence. Occasionally associated with sphalerite beds of both colours are concretions of the same coarse grained sulphides, often with centres of grey dolomitic silt material.

The bedding within the entire zinc-bearing intersections is often mildly disturbed and slumped and this is considered to be a reflection of the same earthquake shocks which produced the heavy slumping, sliding and turbidite deposition in the mineralized beds of the H.Y.C. sub-basin.

COOLEY DOLOMITE MEMBER — GEOLOGY AND MINERALIZATION

Geology

Drilling around the north and east of the H.Y.C. sub-basin shows that a thick sequence of contemporaneously brecciated massive dolomites replaces the pyritic and bituminous shale sequence within distances of as little as 300 m. Northern holes show rapid interfingering of pyritic shales and dolomitic breccias. Here, the presence within the H.Y.C. sequence of wedge-like turbidite breccias comprised of blocks of massive dolomites and algal colony material derived from the Cooley Dolomite Member, suggests a fore-reef and reef relationship. The eastern junction between the H.Y.C. and Cooley Dolomite Members is seen as being of a similar type with later faulting superimposed.

Diamond drilling within the Cooley Dolomite Member has been restricted largely to the western reef flank area and to its eastern sub-outcrop edge where it abuts the main Emu Fault line. Material of obvious algal origin is not frequent in the western holes, but in some eastern holes thick sections of stromatolite colony material can be seen in drill core. Algal debris and oncolites are recorded frequently in petrographic work (Croxford and Jephcott, 1970). The massive dolomites have undergone varying degrees of intraformational brecciation. Matrix material, where in significant quantities, is usually dolomitic mud. Pyritic and bituminous muds do occur occasionally and are most prevalent in the western holes adjacent to the H.Y.C. Pyritic Shale Member.

Mineralization

Two significant bodies of sulphide mineralization have been defined in each of the western and eastern areas. In the former, a broad zone of predominantly diffuse zinc mineralization is known as the Ridge I deposit. Immediately to the south lies a body of lead and minor copper mineralization known as Ridge II. In the east, Cooley I and Cooley II are discrete lead and copper deposits respectively. The deposits are poorly outlined as yet and are of minor importance when compared on a tonnage basis with the nearby H.Y.C. deposit.

The mineralogy is relatively simple. In the two Cooley deposits, sulphides consist of medium to coarse grained galena sphalerite chalcopyrite marcasite pyrite and occasional tetrahedrite. Gangue minerals are ferroan dolomite, quartz and occasionally barytes. The mineralogical associations are generally simple but there are some intricate sulphide-in-sulphide and sulphide-in-gangue relationships usually indicative of diagenetic recrystallization. As far as can be determined from drill core evidence, it appears that the sulphides occur within the massive brecciated dolomite only in open space structures, ranging in thickness from minute cracks through to bodies several centimetres thick; rare masses of sulphides considerably larger than this have been encountered. It is difficult to guess the probable shape and habit of these massive bodies of sulphides but relationship to both tectonic and intraformational brecciation can be inferred.

The Ridge deposits are of a slightly different character, the sulphide mineralization being clearly associated with the matrix of the intraformational dolomite breccias. This matrix is commonly a dark featureless dolomitic material, but in mineralized sections it is often a pyritic shale in which contorted bedding traces are still visible. The sulphides occur as irregular masses or as fine disseminated crystals throughout the matrix. More rarely they rim breccia fragments, or, associated with coarse dolomite crystals, they

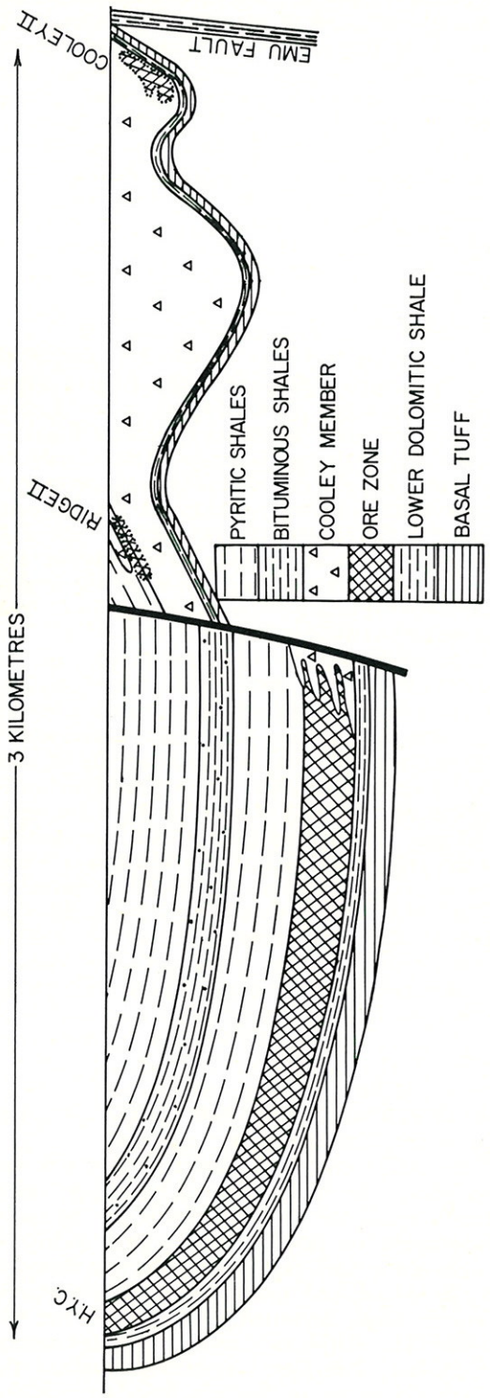

FIG. 4—Idealized cross section through H.Y.C., Ridge and Cooley orebodies.

fill fractures which transgress both the dolomites and the matrix.

Some Ridge II ore is bedded in uncontorted pyritic shales immediately overlying the massive dolomites (Fig. 4). The shales are heavily sheared along their basal contact and the relationship of this ore to that of the H.Y.C. is not clear. It is of note, however, that both the bedded sulphides and carbonates here are coarser in texture than those of the main orebody and it is problematical whether they could represent an upward continuation of the H.Y.C. beds.

CONCLUSIONS

The deposits fall into two main groups—the syn-syngenetic deposits of the H.Y.C. Pyritic Shale Member and the endo-syngenetic deposits of the Cooley Dolomite Member (a classification adapted from Amstutz, 1964). Both were deposited contemporaneously with their respective hosts, but the endo-syngenetic deposits were reorganized by later mechanisms, producing rock and ore associations which suggest similarities to various types of the Mississippi Valley deposits.

From an information source virtually restricted to drill cores, firm statements or opinions on the more theoretical aspects of origin, method of deposition and evolution of the several types of deposits are clearly premature. However some comment is offered in view of the widening fields of syngenetic theory. In the case of the bedded deposits of the H.Y.C. Pyritic Shale Member the concept of a syngenetic origin hardly will excite any argument. The case for syn-syngenetic classification, however, lies in the fact that ore bearing muds at the actual water-sediment interface have taken part in penecontemporaneous deformation in the form of different types of small scale load casting and bottom scouring. This imposes definite limits on ore depositional mechanisms and presents difficulties for those dependent on connate or circulating solutions, or diagenetic formation at any significant depth in the sediment column.

The lack of any metamorphism or sulphide mobilization implies that todays ore grades represent those of the original bottom muds. The method of deposition consequently must be one capable of producing micro-beds of almost pure sulphide. It seems logical to infer that the sea water supplied the metal ions and the sediments the sulphide radicle—giving metal sulphide, either directly by interaction with H_2S supplied by sulphate reducing bacteria, or via an intermediate metal concentrating-biogenic precipitating stage. The latter warrants consideration because changes in respective groups of biogenic populations could provide an explanation for the cyclic changes of ore ratios in "stacked" deposits, and a varying tolerance of particular groups to depth factors could explain the common lead-zinc-iron outward zoning of individual orebodies.

The ultimate source of the metal ions is not clear. As at Mount Isa there is an association with vulcanicity which, apart from providing the trigger mechanism for slump and turbidite movements in the form of earth shocks, may also have provided the metal source via thermal springs. A submarine spring invoking a Salton Sea type source is an alternative possibility; however, the build up of a Red Sea type brine pool appears problematical—a relatively shallow water depth is envisaged for the H.Y.C. sub-basin and the frequent disruptive effects of turbidity flows must be considered.

In the case of the endo-syngenetic deposits of the Cooley Dolomite Member, these are visualized as originating as sulphide muds of differing compositions within the lagoons and deeper pools of the adjoining reefal environment. The breakdown of biostromal formations and shifting carbonate mudbanks caused the entrapment of these muds as thin lens-like pockets in the host dolomite. With burial and contemporaneous brecciation of the enclosing dolomite, the still hydroplastic sulphide bearing material has been redistributed as a breccia matrix. A later and final phase of further re-distribution into open fractures and breccia space along with recrystallization has resulted in coarse grained sulphide-gangue relationships. This last process has been more strongly developed in the Cooley orebodies than in those of the Ridge area and could be due to diagenetic chemico-bacterial reactions in the more porous reefal sections.

ACKNOWLEDGEMENTS

Thanks are due to the management of M.I.M. Holdings Limited and Carpentaria Exploration Company Pty. Ltd. for permission to publish this paper, and the author would like to express his indebtedness to the many geologists who have carried out the detailed work on the region and its orebodies, over the past several years, on which this summary is based.

REFERENCES

Amstutz, G. C., 1964 (ed.). *Sedimentology and Ore Genesis.*

Brown, M. C., 1969. The Proterozoic Barney Creek Formation and H.Y.C. lead-zinc deposit and some associated carbonate units, McArthur Group, McArthur River area N.T., *Rec. Bur. Miner. Resour. Geol. Geophys. Aust.* No. 1969/145.

Cotton, R. E, 1965 H.Y.C. lead-zinc-silver ore deposit, McArthur River in *Geology of Australian Ore Deposits* (Ed. J. McAndrew), pp 197-200 (8th Empire Mining Metallurgical Congress: Melbourne).

Croxford, N. J. W., 1968. A mineralogical examination of the McArthur River lead-zinc-silver deposit, *Proc. Australas. Inst. Min. Metall.*, 226: 97-108.

Croxford, N. J. W. and Jephcott, S., 1972. The McArthur lead-zinc-silver deposit, N.T., *Proc. Australas Inst. Min. Metall.*, 243: 1-26.

Munt, A. D., and Rawlins, R. J., 1966. McArthur Annual Report, Carpentaria Exploration Company Pty. Ltd. Tech. Rep. No. 103 (unpublished).

Shaw, J. A., 1967. McArthur Annual Report, Carpentaria Exploration Company Pty. Ltd. Tech. Rep. No. 139 (unpublished).

Smith, J. W., 1964. Bauhinia Downs N.T., 1:250 000 Geological Series, *Explan. Notes Bur. Miner. Resour. Geol. Geophys. Aust.*, SE/53-3.

REDBANK COPPER DEPOSITS

by G. R. ORRIDGE[1] and A. A. C. MASON[2]

SITUATION, TOPOGRAPHY, HISTORY

Redbank is situated at approximately long. 137°46′E, lat. 17°11′S in the Northern Territory. It is 640 km by road north-north-west from Mt. Isa and 80 km in a direct line from the Gulf of Carpentaria. An annual rainfall of about 72 cm gives rise to well-wooded savannah with permanent water holes along the main drainages. Topography is moderately rugged with south and east facing escarpments up to 130 m high formed by gently dipping, resistant sandstone and lavas.

First discoveries of copper were made in 1912 at Packsaddle and Bauhinia lodes 17 km to the east of Redbank. In 1916 W. Masterton located copper stained outcrops at Redbank and he worked this and the neighbouring Azurite deposit on a small scale until recent years. Workings were confined to shallow pits and shafts in supergene ore containing copper carbonates, chrysocolla and chalcocite. Several mining companies inspected the property in the years 1940 to 1967 and H. J. Jensen (1940) reported on geophysical and geological investigations by AGGSNA. It was not until Harbourside Oil N.L.

1 Supervising Geologist (Mt. Isa) Newmont Pty. Ltd.
2 Engineernig Director, Newmont Pty. Ltd.

APPENDIX C – Geophysical Response of the HYC Deposit

Shalley, M.J, and Harvey, T.V, (1992) Geophysical Response of the HYC Deposit, Exploration Geophysics, Volume 23, p299-304

Exploration Geophysics (1992), **23**, 299–304

Geophysical responses of the HYC Deposit

M. J. Shalley
MIM Exploration Pty Ltd
GPO Box 1042
Brisbane QLD 4001

T. V. Harvey
10 Tiparra St
Eden Hills SA 5050

Abstract

The HYC deposit was discovered in the McArthur River area of the Northern Territory in 1955. Although surface expression is very limited, it was essentially an outcrop discovery resulting from drilling under a small, zinc-rich, siliceous dolomite outcrop. The deposit is described as a sediment-hosted stratiform sulphide. It lies at the base of the Barney Creek Formation in Proterozoic sedimentary rocks of the McArthur Group. The resource is estimated to contain 227 Mt, grading 9.2% Zn, 4.1% Pb, 4.1 g/t Ag and 0.2% Cu.

The body lies beneath a black-soil plain in the McArthur River valley so, while geophysics played no part in the initial discovery, it became an important element in the detailed exploration of the deposit and of the surrounding areas. Induced polarization/resistivity was successful in outlining the HYC deposit and it led to the discovery of new mineralization in the Ridge and Cooley areas. The gravity signature of the deposit is complicated by structure and carbonate rocks, but the method was used successfully to locate a new zone of massive sulphide — unfortunately pyrite only. Early EM methods tested in the area were unsuccessful, but the more recently developed TEM systems have given excellent results, both in profiling and sounding modes. Both the Geotem and Questem airborne systems produce clear anomalies over the deposit. The HYC mineralization has no magnetic signature, but regional airborne magnetics delineates structures, including the Emu Fault, which may be important in the localization of the deposit. A trial seismic reflection line showed some structural elements of the deposit.

Key words: HYC Deposit, Induced polarization, Resistivity, Gravity, Transient EM, Airborne magnetics, Questem, Geotem, INPUT

Introduction

The HYC deposit is a large, sediment-hosted stratiform zinc/lead/silver deposit situated in the Northern Territory at about Latitude 16°26′S and Longitude 136°06′E. The resource contains 227 Mt of ore, grading 9.2% zinc, 4.1% lead, 41 g/t silver and 0.2% copper (Logan *et al.*, 1990). The first indication of the deposit — a silicified dolomite outcrop containing white crystals of hemimorphite — was discovered in 1955. Most of the surrounding area is soil covered. Two drill holes tested the outcrop in 1959. Initial results were disappointing, but the extremely fine grained mineralization of the HYC deposit was subsequently recognised near the bottom of both holes (Logan *et al.*, 1990).

Following the drilling of a third hole 300 m along strike, the significance of the discovery was realised and a program of detailed exploration, including geophysics and geochemistry, was commenced.

Geological and regional geophysical setting

The HYC deposit lies in the Batten Trough in Middle Proterozoic McArthur Group sedimentary rocks. Rock types are mainly carbonates with lesser amounts of sandstone and shale. The mineralization is hosted by the Barney Creek Formation and contained within the HYC Pyritic Shale Member. It is stratiform and very fine-grained. Smaller deposits of coarse-grained disseminated sulphide (lead and zinc and in one case, copper) occur nearby in Cooley Dolomite and Emmerugga Dolomite (Williams, 1978). They are Ridge 1, Ridge 2, Cooley 1 and Cooley 2 (Fig. 1a).

The eastern margin of the system appears to be the Emu Fault. The main elements of mineralization and structure are illustrated in Fig. 1a. A section through the HYC deposit, and selected geophysical profiles, are shown in Fig. 2. The deposit lies on a N-S trending regional gravity high (Fig. 3) and on a deep-sourced local magnetic high (Fig. 4). The Emu Fault Zone is marked by a linear magnetic trend, with contributions from several sources.

Summary of geophysical exploration

Geophysical work began in 1960 with tilt-angle frequency-domain electromagnetics (FEM), self potential and ground magnetics. None of them contributed much. A local gravity survey defined a weak anomaly over the known subcrop. A major advance began with the introduction of induced polarization (IP) and resistivity in 1964. These methods defined the subcrop of the HYC deposit and the broader pyritic basin. They also contributed to the discovery of new mineralization in the Ridge and Cooley deposits. Logging of selected drill holes in 1966 provided additional information. Results are discussed in more detail below.

IP/resistivity soundings, also conducted in 1966, were not helpful. Interpretation of the data produced poor agreement with the known geological section, probably because of strong lateral changes in the geology.

Airborne magnetics began in 1966, and additional data have been accumulated since. The mineralization has no magnetic signature but the regional coverage contributes to structural interpretation (Fig. 4). An airborne FEM survey was flown in 1966, operating at the frequencies 400 Hz and 2300 Hz. It picked up the subcrop of the HYC basin but confident interpretation of bedrock conductors was not possible. The line spacing of 1.6 km was intended for reconnaissance and was not suitable for detailed interpretation. A test Induced-Pulse Transient (INPUT) survey was flown over the deposit by Geoterrex in 1979. This showed a clear anomaly over subcrop and a broader anomaly further to the east (probably Upper Pyritic Shale).

Magnetic induced polarization was applied in 1979, mainly over dolomitic rocks, in the search for more coarse-grained disseminated mineralization. The method appeared to lack penetration and was not particularly selective in terms of sulphide grade. A semi-regional gravity survey was completed over part of the deposit and areas to the north in 1979-80. It

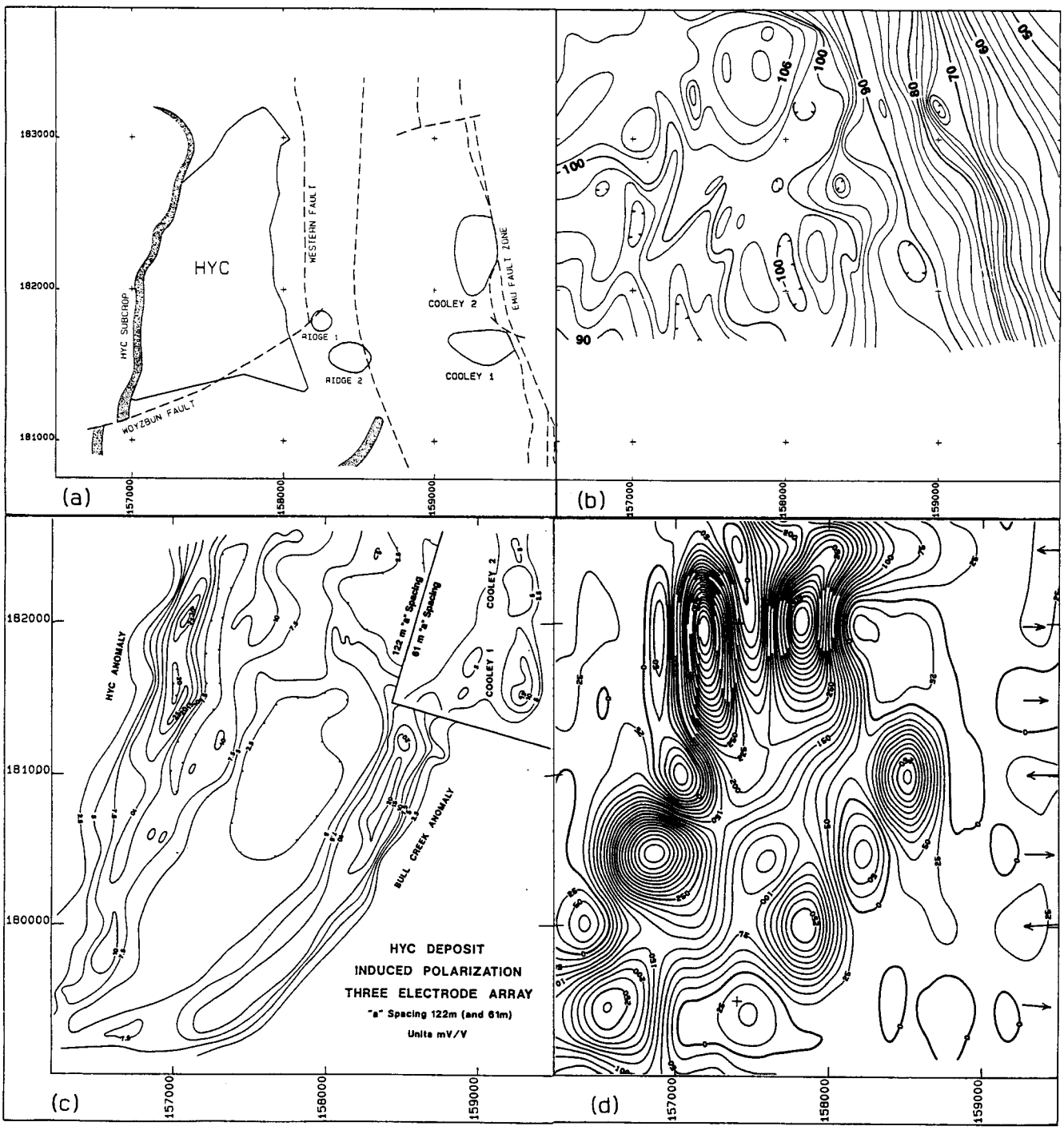

FIGURE 1
Mineralization and geophysical response and anomaly maps, HYC area (Grid units: metre)
(a) Main elements of mineralization and structure
(b) Bouguer gravity anomalies
(c) Induced polarization response (mV/V)
(d) Questem Channel 10 response (ppm)

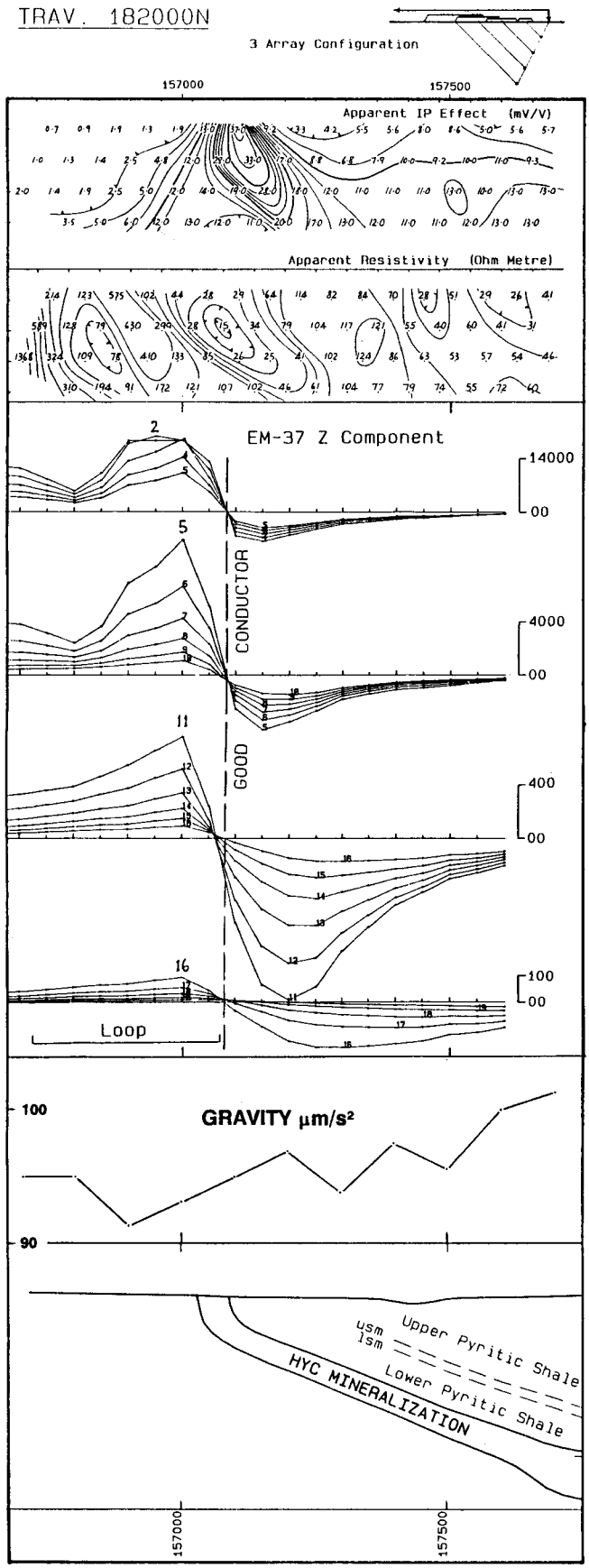

FIGURE 2
Traverse 182 000N geophysical profiles and geological section (Grid units : metre, EM-37 units : nV/Am^2).

defined subcrop reasonably well, but overall results were dominated by rock-type anomalies. Results are discussed below.

In 1982 a test survey using the transient EM system EM-37 was conducted by BHP. A fixed-loop profile across the subcrop gave excellent definition of a conductor and an indication of the dip of the body. Soundings provided interpretable results with good penetration and general agreement with known geology. Results are discussed below. In the same year BHP also conducted a Mini-Sosie seismic reflection test on a 1-km line over the deep section of the HYC deposit and adjacent fault zone. The results suggested that units within the HYC sequence generated consistent reflections, and that the known major faults clearly disrupt this pattern. No detailed interpretation of the data has been attempted.

In 1983 a test audio-magneto-telluric survey was conducted as part of an AMIRA-sponsored equipment-development and test program. Interpreted sections did not agree well with known geology. The results may contain information on deeper structure.

Two test lines of Geotem were flown across the deposit in 1990, and a Questem survey was completed over the deposit and environs in 1991. Both methods detected strongly anomalous responses over the HYC subcrop and adjacent pyritic shales. The broader Questem survey also provided excellent definition of the limits of the pyritic basin (Fig. 1d). Results are discussed below.

Induced polarization and resistivity

The HYC orebody and environs were included in an extensive program of variably spaced 3-array IP/resistivity surveying undertaken at McArthur River from 1964 to 1971. Station locations and dipole measurements were in the imperial units of the day (feet) but have been converted here to metres. The three-array configuration with associated plotting points is illustrated in Fig. 2. Systematic surveying was carried out with dipole spacings of 61 m, 122 m, 183 m and 244 m, surveyed on 244 m, spaced lines; spacings of 30 m, 305 m, 366 m, 427 m, 488 m and 610 m were variously used on sections of some lines.

The ASARCO time-domain IP equipment employed in this program measured the IP voltage 0.75 s after switch-off of a single 4 s pulse. The polarity of successive pulses was manually reversed, and pairs of repeat readings were taken until a satisfactory average had been obtained. Readings were normalized by division by primary voltage and reported as mV/V. Despite the primitive nature of the equipment, the data appear to be of good quality.

This IP/resistivity survey outlined several zones of anomalous IP effects, variously associated with locally higher and lower resistivities. The IP response is shown in Fig. 1c. This map extends further south than the accompanying geological map and covers the southern extension of the pyritic basin. The dominant feature is an extensive, apparently folded zone of strongly anomalous IP effects and associated lower

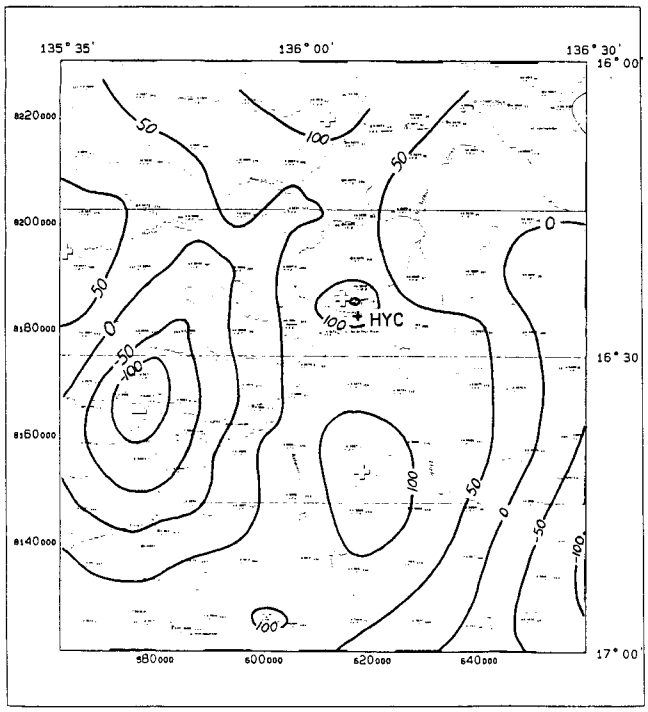

FIGURE 3
Regional Bouguer anomaly gravity map, McArthur River Region (After BMR) (Units : $\mu m/s^2$).

resistivities. The position and extent of the HYC orebody outcrop and subcrop coincide with the peak development of the western 'limb' of this zone. Drill testing elsewhere along the IP anomaly has shown the source to be pyritic shales.

The typical response of the HYC orebody is illustrated in the apparent resistivity and IP effect pseudosection shown in Fig. 2. The IP/resistivity traverse, done on an earlier grid, lies at an angle of 19° clockwise from the current grid. It is projected onto Traverse 182 000N and crosses it at 157 000E.

The outcrop position of the orebody corresponds to a very strong, shallow-sourced IP anomaly and approximately coincident low resistivity zone. To the west, the very low background IP effects and generally high resistivities reflect unmineralized dolomitic footwall rocks. To the east, the somewhat anomalous IP effects and intermediate resistivities reflect the pyritic, dolomitic hanging wall sequence. The disseminated sulphide deposits (Ridge and Cooley) coincide with weak to moderate IP anomalies. Cooley 2 is also weakly conductive.

IP measurements made on selected core samples confirm the strongly anomalous nature of the ore and adjacent pyritic material. An IP/resistivity log of DDH N20/62D, read with a 6.1-m two-electrode array, is shown in Fig. 5. The log shows that the HYC mineralization and the overlying pyritic shale are both moderately conductive and polarizable. Peaks within the IP response tend to correlate with resistivity highs. This hole is located at 157 864E, 182 028N.

No modern, spectral-style IP has been surveyed at McArthur River.

Gravity

The HYC orebody and environs, excluding the southern part of the basin, were covered in an extensive program of gravity surveying carried out at McArthur River in 1979 and 1980. In the central area of interest, gravity stations were read at 100-m intervals (reduced to 50 m in some areas) along 250-m or 500-m spaced east-west lines, and 200-m or 400-m spaced north-south lines. Results of part of the survey are presented in Fig. 1b. The dominant feature in the gravity results is a very strong gradient of about $-50\ \mu m\ s^{-2}\ km^{-1}$ towards the east-north-east, on the eastern side of the area. This feature coincides, in strike direction and position, with the regional-scale Emu Fault Zone. The source of the gravity gradient is attributed to the density contrast between mainly dolomitic (more dense) rock types to the west of the fault, and mainly clastic (less dense) rock types to the east.

Detailed assessment of the gravity results shows a small but persistent gravity high (4 to 5 $\mu m/s^2$ amplitude), roughly coincident with the subcrop position of the HYC orebody (Figs 1a, 1b and 2). However, this feature is not unique; other similar anomalies in the area can be related to dolomitic units and dolomitised zones, etc. A broad gravity high covers the HYC deposit but is not uniquely associated with it. Extension of the high to the northwest is attributed to dolomitic rocks. The eastern margin of the high is controlled more by the Emu Fault gradient than by the eastern edge of mineralization.

Detailed modelling of the results was aimed at analysing the peak gravity high at 157 900E, 183 700N. After stripping away regional effects and the response from dolomitic rocks, an unexplained residual anomaly remained. It was tested by

FIGURE 4
Grey-scale image of composite BMR and detailed total-field magnetic data set, McArthur River Region (Illumination from N.W.)

drilling, which revealed a thick section of moderately to heavily pyritic sediments in the depth range 405 m to 598 m.

Extensive density measurements have been carried out on surface and underground rock samples, and on drill cores. The results confirm the high density of the ore zone (average range 3.2 to 3.3 t/m^3), and the density contrast between dolomitic units (average range 2.7 to 2.9 t/m^3) and clastic units (average range 2.4 to 2.7 t/m^3).

Time-domain electromagnetics

In July 1982, with the permission of Carpentaria Exploration Company Pty Ltd, BHP conducted a test of the EM-37 time-domain EM system over the deposit. The test comprised both fixed-loop traverses and depth soundings at selected locations. EM-37 is an impulse type time-domain system described by McNeill (1980). More general descriptions of the time-domain EM method are widely reported in the literature (e.g. Buselli and O'Neill, 1977). The base frequency for the survey was 25 Hz.

A fixed-loop traverse was conducted over the subcrop on Line 182 000N using a 600 m x 350 m transmitter loop. Loop current and turn-off times were about 15 A and 300 μs respectively. Loop position and Z-component results are presented, together with a geological section, in Fig. 2. A clear 'cross-over' response is closely associated with the subcrop of the deposit.

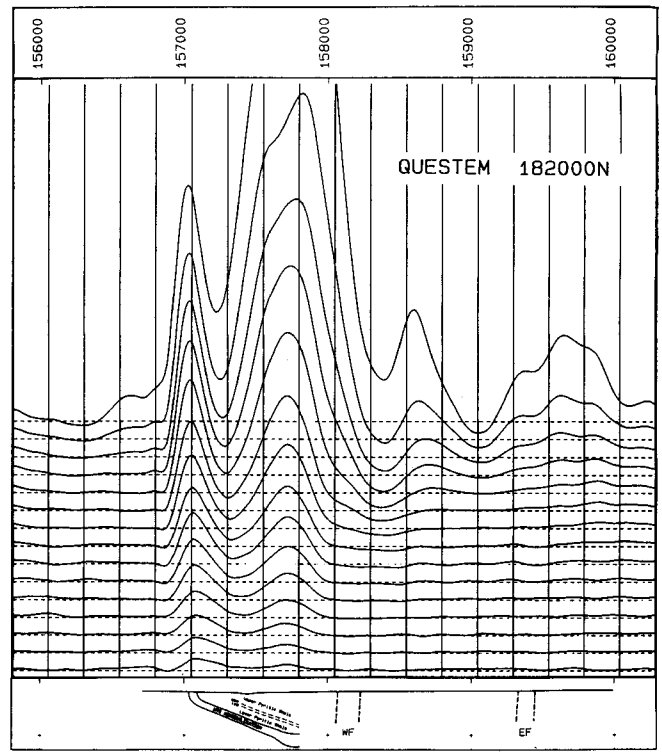

FIGURE 6
Traverse 182 000N Questem profile and geological section (Grid units : metre, WF = Western Fault, EF = Emu Fault).

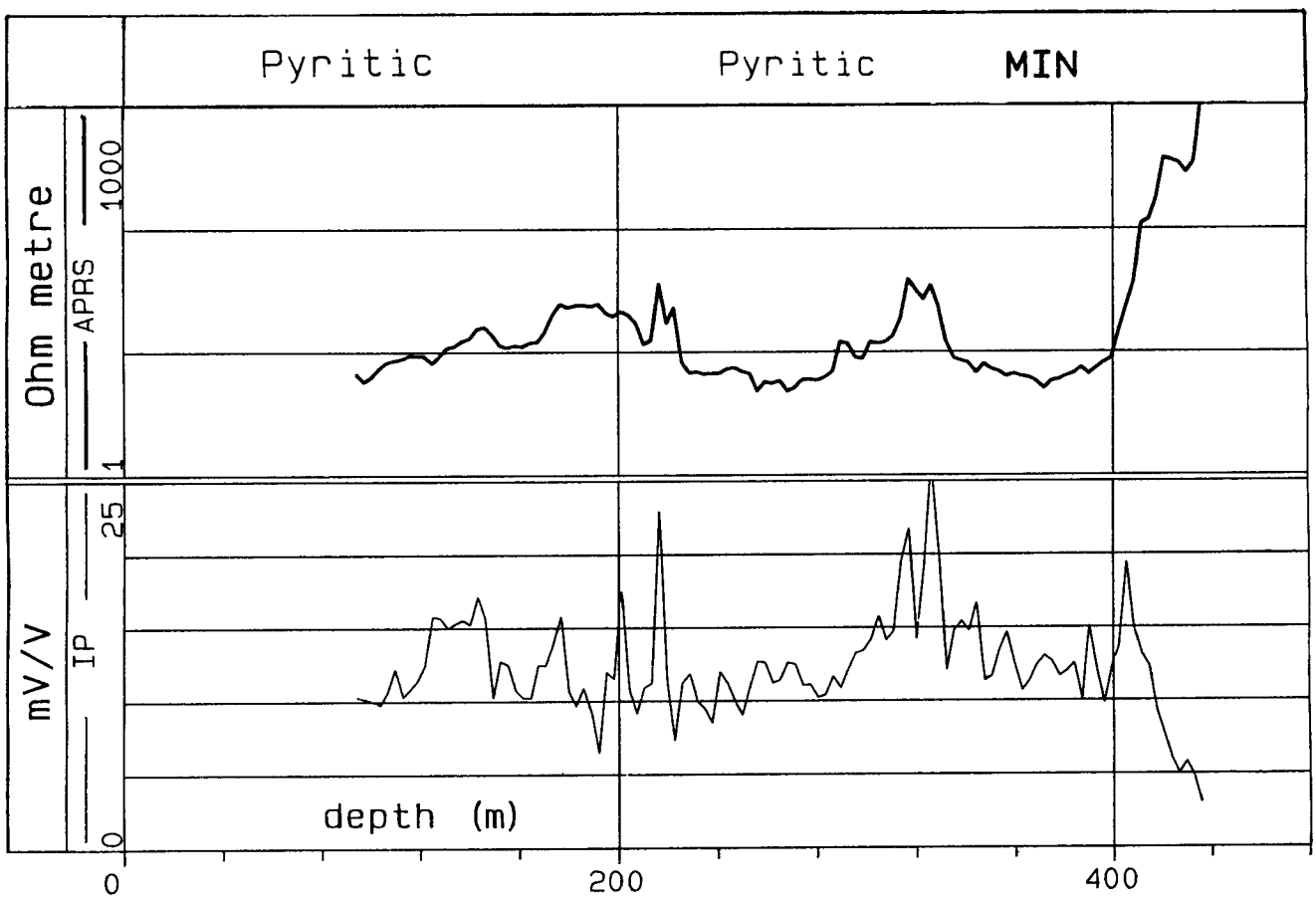

FIGURE 5
Induced polarization and apparent resistivity log, DDH N20/62D

The response has some interesting characteristics which can be explained in terms of the geological section. In detail we see that, at early times, the positive peak of the profile is dominant. At later times the negative peak becomes progressively stronger and eventually dominant. It also becomes much broader, and the peak migrates to the east. The early-time positive peak is due in part to the subcrop of the body, which is reasonably broad (about 60 m). The conductor may be broader still if pyritic shale is included. A relatively strong contribution can therefore be expected from horizontally disposed eddy currents inside the transmitter loop at early times. At intermediate times, the response from eddy currents in the plane of the orebody should dominate, and we see the 'cross-over' profile typical of a steeply dipping body. The increasingly strong negative peak at later times, and the broadening and migration of the peak, indicate flattening of the body to the east. There also seems to be some minor wandering of the 'cross-over' point, the reason for which we do not understand.

Several soundings were conducted with loop sizes varying from 200 m to 400 m square. Z-component readings were taken at the centre of the loop and, in some cases, outside the loop, to check for the so called 'loop effect' (Asten and Price, 1985). Interpretation of the soundings, using layered-earth inversion software, produced reasonably good agreement with known geology (Asten and Price, 1985).

Questem and Geotem

Questem and Geotem are both time-domain airborne EM systems which use a half-sine-wave energising current in a multiturn transmitter loop mounted on a fixed wing aircraft. The horizontal axis receiver is carried in a towed 'bird' and measures secondary signal at selected time channels between transmitter current pulses. The Questem survey was flown over the deposit and environs in 1991 with the following operating parameters:

Flight Line Direction:	90°/270°
Flight Line Spacing:	500 m
Mean Terrain Clearance:	120 m
Mean Sensor Height:	45 m
Base Frequency:	75 Hz
Receiver Channels:	15 channels from 0.247 to 4.205 ms

The Channel 10 (1.861 ms) contour map for the part of the survey which covers the HYC deposit, and the southern extent of the pyritic basin, is shown in Fig. 1d. Note the very good agreement between the Questem and the induced polarization in defining the HYC subcrop and the southern extent of the basin (Figs 1c, 1d). The bullseye effect in the Questem contours is caused by the alternating flight directions of the survey. A broader anomaly east of the subcrop is due mainly to pyritic shale but may have some contribution from the low-dipping deeper mineralization. A Questem profile on Traverse 182 000N is shown in Fig. 6 with a geological section.

The Geotem survey flown in 1990 was restricted to two test lines with the following operating parameters:

Flight Line Direction:	90°/270°
Mean Terrain Clearance:	20 m
Mean Sensor Height:	54 m
Base Frequency:	125 Hz
Receiver Channel:	12 channels from 0.369 ms to 2.556 ms

Both the Geotem and Questem surveys flew an identical West to East traverse on 182 000N. The results are very similar.

Conclusions

The HYC deposit and associated pyritic basin emerge from this study as conductive, polarizable and relatively dense. The presence of pyritic shale complicates the application of geophysical methods but also presents a larger target to exploration. Dolomites and dolomitic sediments appear to have a greater influence on gravity than the pyritic and mineralized beds, but the latter do produce a gravity signature.

Acknowledgements

Results reported here are the work of many geophysicists, geologists and support staff over a period of thirty-two years. The authors wish to thank the management of M.I.M. Exploration Pty Ltd for permission to publish the paper, and current geological staff, Ross Logan, Dugi Wilson and Matt Williams, for their help and support in assembling the data.

References

Asten, M. W., and Price, D. G. (1985). 'Transient EM soundings by the in/out-loop method.' *Explor. Geophys.* **16**, 165-168.

Buselli, G., and O'Neill, B. (1977). 'SIROTEM: A new portable instrument for multichannel transient electromagnetic measurements.' *Aust. Soc. Explor. Geophys. Bull.* **8**, 82-87.

McNeill, J. D. (1980). 'EM-37 ground transient electromagnetic system: calculated depth of exploration.' Geonics Ltd Technical Note TN-10.

Logan, R. G., Murray, W. J., and Williams, N. (1990). 'HYC Silver-Lead-Zinc Deposit, McArthur River.' *In* 'Geology of the Mineral Deposits of Australia and Papua New Guinea' Vol. 1 (F. E. Hughes ed.). Aust. Inst. of Mining and Metallurgy, 907-911.

Williams, N. (1978). 'Studies of the base metal sulphide deposits at McArthur River, Northern Territory, Australia : I. The Cooley and Ridge Deposits.' *Econ. Geol.* **73**, 1005-1035.

APPENDIX D – Geotech Survey Report

SURVEY AND LOGISTICS REPORT ON A HELICOPTER BORNE VERSATILE TIME DOMAIN ELECTROMAGNETIC (VTEM) SURVEY

on the

CARANBINI AREA

AUSTRALIA

for

BRUMBY RESOURCES LIMITED

by

GEOTECH AIRBORNE PTY LTD

Unit 1, 29 Mulgul Road
Malaga, WA, 6090,
Australia
Tel: +61 8 9249 8814
Fax: +61 8 9249 8894
www.geotechairborne.com
e-mail: info@geotechairborne.com

Project AA911
December, 2010

TABLE OF CONTENTS

APPENDICES

SURVEY AND LOGISTICS REPORT ON A HELICOPTER-BORNE VTEM SURVEY

1. SURVEY SPECIFICATIONS

1.1. General

Job Number	*AA911*
Client	*Brumby Resources Limited.*
Project Area	*Caranbini Area*
Location	*Australia*
Number of Blocks	*1*
Total line kilometres	*904km*
Survey date	*18 - 21 November, 2010*
Client Representative	*John Ikstrums* *Tel: +61 8 9486 8333* *Fax: +61 8 9322 5123* *Email: john@brumbyresources.com.au*
Client address	*Unit 3, 49 Ord Street* *West Perth, WA 6005, Australia*

1.2. VTEM flight plan on Google EARTH™ Background

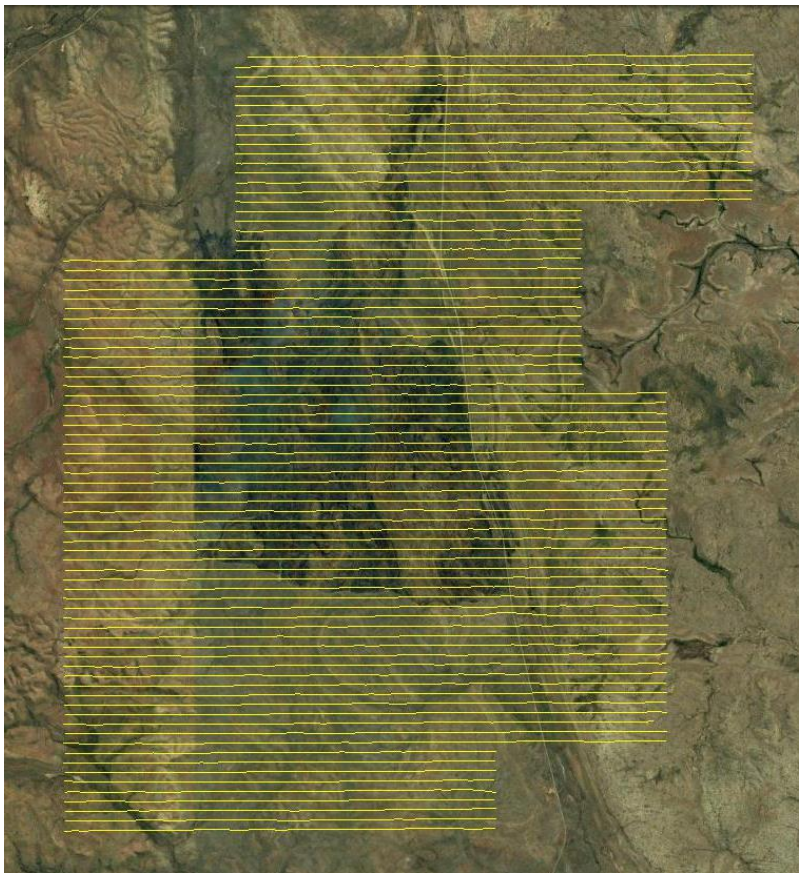

1.3. Survey block coordinates.

Easting UTM Z 53S	Northing UTM Z 53S
Caranbini Area	
610440.83	8206365.81
621129.80	8206311.23
621111.92	8203079.02
617549.73	8203094.91
617529.57	8199407.09
619310.52	8199397.44
619270.13	8192021.73
615709.46	8192040.97
615699.64	8190197.06
606798.86	8190242.66
606857.25	8202152.05
610419.48	8202134.35
610440.83	8206365.81

1.4. Survey block specifications

Survey block	Line spacing (m)	Line-km (contractual)	Line-km (delivered)	Flight direction	Line number
Caranbini	200	898	904	090-270	L10010 – L10810

1.5. Survey schedule

Date	Flight #	Block	Nominal Production Km flown	Comments
18-Nov-10	1-4	Caranbini	220	Production
19-Nov-10	5-7	Caranbini	178	Production
20-Nov-10	8-12	Caranbini	352	Production
21-Nov-10	13-15	Caranbini	156	Production

2. SYSTEM SPECIFICATIONS

2.1. Instrumentation

Survey Helicopter	
Model	*Augusta AW119-KE*
Registration	*VH-KEJ*
Nominal survey speed	*80 km/h*
Nominal terrain clearance	*88 m*
VTEM Transmitter	
Coil diameter	*35 m*
Number of turns	*4*
Pulse repetition rate	*25 Hz*
Peak current	*226 Amp*
Duty cycle	*28.67%*
Peak dipole moment	*870,099 NIA*
Pulse width	*5.74 ms*
Nominal terrain clearance	*34 m*
VTEM Receiver	
Coil diameter	*1.2 metre*
Number of turns	*100*
Effective area	*113.1 m^2*
Sampling interval	*0.1 s*
Nominal terrain clearance	*42 m*
Magnetometer	
Type	*Geometrics*
Model	*Optically pumped cesium vapour*
Sensitivity	*0.02 nT*
Sampling interval	*0.1 s*
Cable length	*13 m*
Nominal terrain clearance	*78 m*
Radar Altimeter	
Type	*Terra TRA 3000/TRI 40*
Position	*Beneath cockpit*
Sampling interval	*0.2 s*
GPS navigation system	
Type	*NovAtel*
Model	*WAAS enabled OEM4-G2-3151W*
Antenna position	*Helicopter tail*
Sampling interval	*0.2 s*
Base Station Magnetometer/GPS	
Type	*Geometrics*
Model	*Cesium vapour*
Sensitivity	*0.001 nT*
Sampling interval	*1 s*

2.2. VTEM Configuration

Configuration	
Cable angle with vertical	35 °
Cable length (EM receiver)	57 m
Cable length (Magnetometer)	13 m

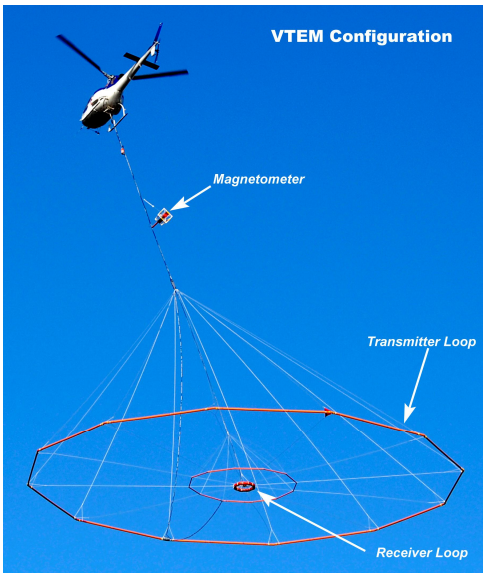

2.3. VTEM decay sampling scheme

B-field VTEM Decay Sampling scheme				
Array	Microseconds			
Index	Middle	Start	End	Width
13	83	78	90	12
14	96	90	103	13
15	110	103	118	15
16	126	118	136	18
17	145	136	156	20
18	167	156	179	23
19	192	179	206	27
20	220	206	236	30
21	253	236	271	35
22	290	271	312	40
23	333	312	358	46
24	383	358	411	53
25	440	411	472	61
26	505	472	543	70
27	580	543	623	81
28	667	623	716	93
29	766	716	823	107
30	880	823	945	122
31	1010	945	1086	141
32	1161	1086	1247	161
33	1333	1247	1432	185
34	1531	1432	1646	214
35	1760	1646	1891	245
36	2021	1891	2172	281
37	2323	2172	2495	323
38	2667	2495	2865	370
39	3063	2865	3292	427
40	3521	3292	3781	490
41	4042	3781	4341	560
42	4641	4341	4987	646
43	5333	4987	5729	742
44	6125	5729	6581	852
45	7036	6581	7560	979
46	8083	7560	8685	1125
47	9286	8685	9977	1292
48	10667	9977	11458	1482

2.4. VTEM Transmitter Waveform over one half-period (November 2010)

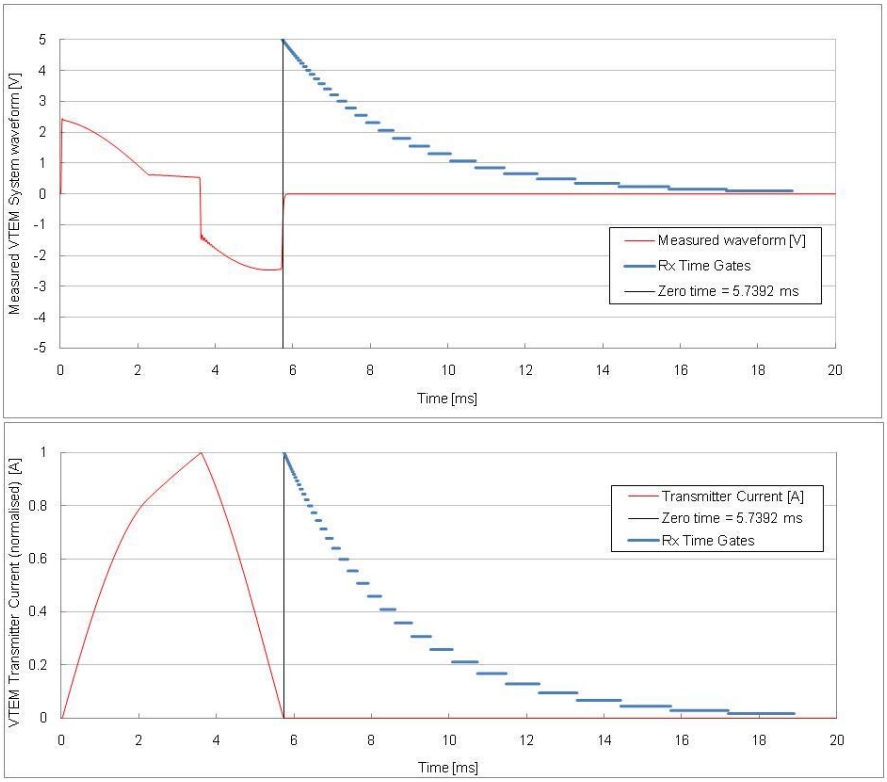

3. PROCESSING

3.1. Processing parameters

Coordinates	
Projection	*MAP GRID AUS ZONE 53*
Datum	*GDA 94*
Spherics rejection (EM and Magnetic data)	
Non-linear filter	*4 point*
Non-linear filter sensitivity	*0.00001*
Low-pass filter wavelength	*20 fids*
Lag correction of other sensors to EM receiver position	
GPS	*25 m*
Radar	*35 m*
Magnetometer	*25.5 m*

3.2. Flight Path

The flight path, recorded by the acquisition program as WGS 84 latitude/longitude, was converted into the UTM coordinate system in Oasis Montaj. The flight path was drawn using linear interpolation between x,y positions from the navigation system. Positions are updated every second and expressed as UTM eastings (x) and UTM northings (y).

3.3. Electromagnetic Data

A three stage digital filtering process was used to reject major sferic events and to reduce system noise. Local sferic activity can produce sharp, large amplitude events that cannot be removed by conventional filtering procedures. Smoothing or stacking will reduce their amplitude but leave a broader residual response that can be confused with geological phenomena. To avoid this possibility, a computer algorithm searches out and rejects the major sferic events.

The signal to noise ratio was further improved by the application of a low pass linear digital filter. This filter has zero phase shift which prevents any lag or peak displacement from occurring, and it suppresses only variations with a wavelength less than the specified filter wavelength.

3.4. Magnetic Data

The processing of the magnetic data involved the correction for diurnal variations by using the digitally recorded ground base station magnetic values. The base station magnetometer data was edited and merged into the Geosoft GDB database on a daily basis. The aeromagnetic data was corrected for diurnal variations by subtracting the observed magnetic base station deviations.

A micro-levelling procedure was then applied. This technique is designed to remove persistent low-amplitude components of flight-line noise.

The corrected magnetic data was interpolated between survey lines using a random point gridding method to yield x-y grid values for a standard grid cell size of a quarter of the line spacing. The Minimum Curvature algorithm was used to interpolate values onto a rectangular regular spaced grid.

3.5. Digital Terrain Model

Subtracting the radar altimeter data from the GPS elevation data creates a digital elevation model.

4. DELIVERABLES

VTEM Survey and logistics report		
Format	PDF	
Database		
Format	Digital Geosoft (.GDB)	
Channels	Name	Description
	X_UTM	X positional data (UTM Z53S / WGS84)
	Y_UTM	Y positional data (UTM Z53S / WGS84)
	X_MGA	X positional data (MGA Z53 / GDA94)
	Y_MGA	Y positional data (MGA Z53 / GDA94)
	Lon	Longitude data
	Lat	Latitude data
	Z	GPS antenna elevation (metres above sea level)
	Radar	Helicopter terrain clearance from radar altimeter (metres above ground level)
	RxAlt	EM Receiver and Transmitter terrain clearance (metres above ground level)
	DTM	Digital terrain model (metres)
	Gtime	UTC time (seconds of the day)
	MagTF	Raw Total Magnetic field data (nT)
	MagBase	Magnetic diurnal variation data (nT)
	MagDiu	Total Magnetic field diurnal variation and lag corrected data (nT)
	MagMicL	Microleveled Total Magnetic field data (nT)
	dBdtZ[13] to dBdtZ[48]	dB/dtZ, Time Gates 83 µs to 10667 µs (pV/A/m^4)
	BfieldZ[13] to BfieldZ[48]	B-fieldZ, Time Gates 83 µs to 10667 µs (pV.ms/A/m^4)
	dBdtX[20] to dBdtX[48]	dB/dtX, Time Gates 220 µs to 10667 µs (pV/A/m^4)
	BfieldX[20] to BfieldX[48]	B-fieldX, Time Gates 220 µs to 10667 µs (pV.ms/A/m^4)
	dBdtX_FF[20] to dBdtX_FF[48]	Fraser Filter dB/dtX, Time Gates 220 µs to 10667 µs (pV/A/m^4)
	BfieldX_FF[20] to BfieldX_FF[48]	Fraser Filtered B-fieldX, Time Gates 220 µs to 10667 µs (pV.ms/A/m^4)
	dBdtX_SFF_20_30	Stacked Fraser Filtered data from channel 20 to 30 (pV/A/m^4)
	BfieldX_SFF_20_30	Stacked Fraser Filtered data from channel 20 to 30 (pV.ms/A/m^4)
	dBdtY[20] to dBdtY[48]	dB/dtY, Time Gates 220 µs to 10667 µs (pV/A/m^4)
	BfieldY[20] to BfieldY[48]	B-fieldY, Time Gates 220 µs to 10667 µs (pV.ms/A/m^4)
	dBdtY_FF[20] to dBdtY_FF[48]	Fraser Filter dB/dtY, Time Gates 220 µs to 10667 µs (pV/A/m^4)
	BfieldY_FF[20] to BfieldY_FF[48]	Fraser Filtered B-fieldY, Time Gates 220 µs to 10667 µs (pV.ms/A/m^4)
	dBdtY_SFF_20_30	Stacked Fraser Filtered data from channel 20 to 30 (pV/A/m^4)
	BfieldY_SFF_20_30	Stacked Fraser Filtered data from channel 20 to 30 (pV.ms/A/m^4)
	PLM	Power line monitor

Grids		
Format	Digital Geosoft (.GRD and .GI)[1]	
Grids	Name	Description
	AA911_Mag	Total Magnetic field (nT)
	AA911_dBdtX_SFF	dBdtX Stacked Fraser Filtered data
	AA911_BfieldX_SFF	BfieldX Stacked Fraser Filtered data
	AA911_dBdtY_SFF	dBdtY Stacked Fraser Filtered data
	AA911_BfieldY_SFF	BfieldY Stacked Fraser Filtered data

Maps		
Format	Digital Geosoft (.MAP)	
Scale	1:25 000	
Maps	Name	Description
	AA911 _Mag	Total Magnetic field colour contours
	AA911_dBdtZ_Log	VTEM dB/dt profiles, Time Gates 0.667 – 10.667 ms in linear - logarithmic scale
	AA911_BfieldZ_Log	VTEM B-field profiles, Time Gates 0.667 – 10.667 ms in linear - logarithmic scale
	AA911_dBdtX_SFF	dBdtX Stacked Fraser Filtered data
	AA911_BfieldX_SFF	BfieldX Stacked Fraser Filtered data
	AA911_dBdtY_SFF	dBdtY Stacked Fraser Filtered data
	AA911_BfieldY_SFF	BfieldY Stacked Fraser Filtered data

Waveform		
Format	Digital Excel Spreadsheet (AA911_VTEM_Waveform.xls)	
Columns	Name	Description
	Time	Sampling rate interval, 10.416 µs
	Volt	Output voltage of the receiver coil (volt)
	Current	Transmitter current (normalised to 1A peak)

Google Earth Flight Path file	
Format	Google Earth AA911_FlightPath.kml
	Free version of Google Earth software can be downloaded from, http://earth.google.com/download-earth.html

[1] A Geosoft .GRD file has a .GI metadata file associated with it, containing grid projection information.

5. PERSONNEL

Geotech Airborne Limited Personnel	
Operator / Crew chief	*Gregory Downs*
Data Processing (Preliminary)	*Pete Holbrook*
Data Processing (Final) /Reporting	*Matt Holbrook*
Final data supervision	*Malcolm Moreton* *Data Processing Manager* *(malcolm@geotechairborne.com)*
Overall project management	*Keith Fisk* *Managing Partner and Director* *(keith@geotechairborne.com)*

APPENDIX A

GENERALIZED MODELING RESULTS OF THE VTEM SYSTEM (by Roger Barlow)

Introduction

The VTEM system is based on a concentric or central loop design, whereby, the receiver is positioned at the centre of a 35 metres diameter transmitter loop that produces a dipole moment up to 870,099 NIA at peak current. The wave form is a bi-polar, modified square wave with a turn-on and turn-off at each end. With a base frequency of 25 Hz, the duration of each pulse is approximately 7.5 milliseconds followed by an off time where no primary field is present.

During turn-on and turn-off, a time varying field is produced (dB/dt) and an electro-motive force (emf) is created as a finite impulse response. A current ring around the transmitter loop moves outward and downward as time progresses. When conductive rocks and mineralization are encountered, a secondary field is created by mutual induction and measured by the receiver at the centre of the transmitter loop.

Measurements are made during the off-time, when only the secondary field (representing the conductive targets encountered in the ground) is present.

Efficient modeling of the results can be carried out on regularly shaped geometries, thus yielding close approximations to the parameters of the measured targets. The following is a description of a series of common models made for the purpose of promoting a general understanding of the measured results.

Variation of Plate Depth

Geometries represented by plates of different strike length, depth extent, dip, plunge and depth below surface can be varied with characteristic parametres like conductance of the target, conductance of the host and conductivity/thickness and thickness of the overburden layer.

Diagrammatic models for a vertical plate are shown in figures A and G at two different depths, all other parametres remaining constant. With this transmitter-receiver geometry, the classic **M** *shaped response is generated. Figure A shows a plate where the top is near surface. Here, amplitudes of the duel peaks are higher and symmetrical with the zero centre positioned directly above the plate. Most important is the separation distance of the peaks. This distance is small when the plate is near surface and widens with a linear relationship as the plate (depth to top) increases. Figure G shows a much deeper plate where the separation distance of the peaks is much wider and the amplitudes of the channels have decreased.*

Variation of Plate Dip

As the plate dips and departs from the vertical position, the peaks become asymmetrical. Figure B shows a near surface plate dipping 80º. Note that the direction of dip is toward the high shoulder of the response and the top of the plate remains under the centre minimum.

As the dip increases, the aspect ratio (Min/Max) decreases and this aspect ratio can be used as an empirical guide to dip angles from near 90º to about 30º. The method is not sensitive enough where dips are less than about 30º. Figure E shows a plate dipping 45º and, at this angle, the minimum shoulder starts to vanish. In Figure D, a

flat lying plate is shown, relatively near surface. Note that the twin peak anomaly has been replaced by a symmetrical shape with large, bell shaped, channel amplitudes which decay relative to the conductance of the plate.

Figure H shows a special case where two plates are positioned to represent a synclinal structure. Note that the main characteristic to remember is the centre amplitudes are higher (approximately double) compared to the high shoulder of a single plate. This model is very representative of tightly folded formations where the conductors where once flat lying.

Variation of Prism Depth

Finally, with prism models, another algorithm is required to represent current on the plate. A plate model is considered to be infinitely thin with respect to thickness and incapable of representing the current in the thickness dimension. A prism model is constructed to deal with this problem, thereby, representing the thickness of the body more accurately.

Figures C, F and I show the same prism at increasing depths. Aside from an expected decrease in amplitude, the side lobes of the anomaly show a widening with deeper prism depths of the bell shaped early time channels.

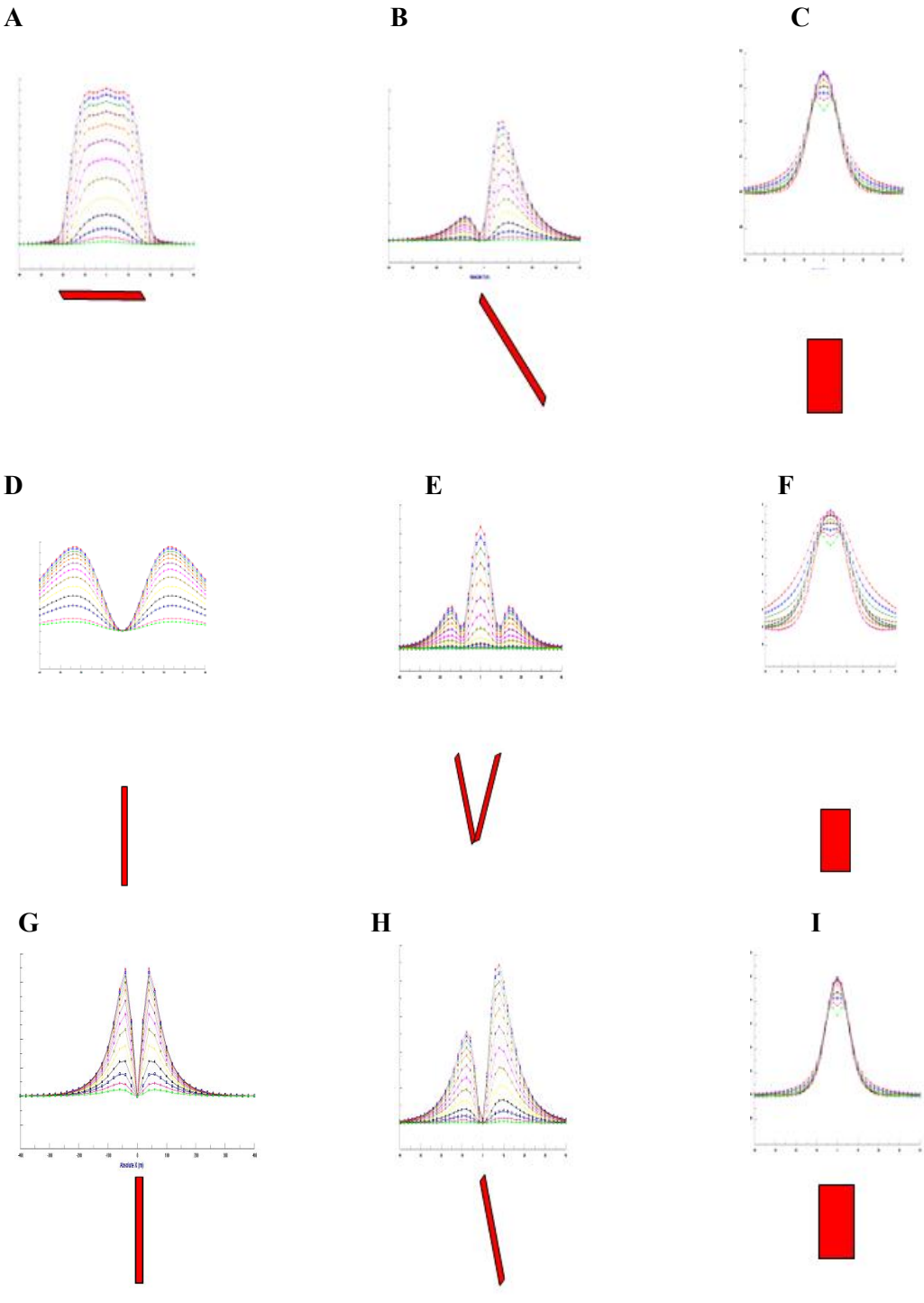
A
B
C
D
E
F
G
H
I

General Modeling Concepts

A set of models has been produced for the Geotech VTEM® system with explanation notes (see models A to I above). The reader is encouraged to review these models, so as to get a general understanding of the responses as they apply to survey results. While these models do not begin to cover all possibilities, they give a general perspective on the simple and most commonly encountered anomalies.

When producing these models, a few key points were observed and are worth noting as follows:

- *For near vertical and vertical plate models, the top of the conductor is always located directly under the centre low point between the two shoulders in the classic* **M** *shaped response.*
- *As the plate is positioned at an increasing depth to the top, the shoulders of the* **M** *shaped response, have a greater separation distance.*
- *When faced with choosing between a flat lying plate and a prism model to represent the target (broad response) some ambiguity is present and caution should be exercised.*
- *With the concentric loop system and Z-component receiver coil, virtually all types of conductors and most geometries are most always well coupled and a response is generated (see model H). Only concentric loop systems can map this type of target.*

The modelling program used to generate the responses was prepared by PetRos Eikon Inc. and is one of a very few that can model a wide range of targets in a conductive half space.

General Interpretation Principals

Magnetics

The total magnetic intensity responses reflect major changes in the magnetite and/or other magnetic minerals content in the underlying rocks and unconsolidated overburden. Precambrian rocks have often been subjected to intense heat and pressure during structural and metamorphic events in their history. Original signatures imprinted on these rocks at the time of formation have, it most cases, been modified, resulting in low magnetic susceptibility values.

The amplitude of magnetic anomalies, relative to the regional background, helps to assist in identifying specific magnetic and non-magnetic rock units (and conductors) related to, for example, mafic flows, mafic to ultramafic intrusives, felsic intrusives, felsic volcanics and/or sediments etc. Obviously, several geological sources can produce the same magnetic response. These ambiguities can be reduced considerably if basic geological information on the area is available to the geophysical interpreter.

In addition to simple amplitude variations, the shape of the response expressed in the wave length and the symmetry or asymmetry, is used to estimate the depth, geometric parameters and magnetization of the anomaly. For example, long narrow magnetic linears usually reflect mafic flows or intrusive dyke features. Large areas with complex magnetic patterns may be produced by intrusive bodies with significant magnetization, flat lying magnetic sills or sedimentary iron formation. Local isolated circular magnetic patterns often represent plug-like igneous intrusives such as kimberlites, pegmatites or volcanic vent areas.

Because the total magnetic intensity (TMI) responses may represent two or more closely spaced bodies within a response, the second derivative of the TMI response may be helpful for distinguishing these complexities. The second derivative is most useful in mapping near surface linears and other subtle magnetic structures that are partially masked by nearby higher amplitude magnetic features. The broad zones of higher magnetic amplitude, however, are severely attenuated in the vertical derivative results. These higher amplitude zones reflect rock units having strong magnetic susceptibility signatures. For this reason, both the TMI and the second derivative maps should be evaluated together.

Theoretically, the second derivative, zero contour or colour delineates the contacts or limits of large sources with near vertical dip and shallow depth to the top. The vertical gradient map also aids in determining contact zones between rocks with a susceptibility contrast, however, different, more complicated rules of thumb apply.

Concentric Loop EM Systems

Concentric systems with horizontal transmitter and receiver antennae produce much larger responses for flat lying conductors as contrasted with vertical plate-like conductors. The amount of current developing on the flat upper surface of targets having a substantial area in this dimension, are the direct result of the effective coupling angle, between the primary magnetic field and the flat surface area. One therefore, must not compare the amplitude/conductance of responses generated from flat lying bodies with those derived from near vertical plates; their ratios will be quite different for similar conductances.

Determining dip angle is very accurate for plates with dip angles greater than 30º. For angles less than 30º to 0º, the sensitivity is low and dips can not be distinguished accurately in the presence of normal survey noise levels.

A plate like body that has near vertical position will display a two shoulder, classic **M** *shaped response with a distinctive separation distance between peaks for a given depth to top.*

It is sometimes difficult to distinguish between responses associated with the edge effects of flat lying conductors and poorly conductive bedrock conductors. Poorly conductive bedrock conductors having low dip angles will also exhibit responses that may be interpreted as surfacial overburden conductors. In some situations, the conductive response has line to line continuity and some magnetic correlation providing possible evidence that the response is related to an actual bedrock source.

The EM interpretation process used, places considerable emphasis on determining an understanding of the general conductive patterns in the area of interest. Each area has different characteristics and these can effectively guide the detailed process used.

The first stage is to determine which time gates are most descriptive of the overall conductance patterns. Maps of the time gates that represent the range of responses can be very informative.

Next, stacking the relevant channels as profiles on the flight path together with the second vertical derivative of the TMI is very helpful in revealing correlations between the EM and Magnetics.

Next, key lines can be profiled as single lines to emphasize specific characteristics of a conductor or the relationship of one conductor to another on the same line. Resistivity Depth sections can be constructed to show the relationship of conductive overburden or conductive bedrock with the conductive anomaly.

APPENDIX B

VTEM X-COMPONENT DATA

6. X COIL DATA

6.1. Sign convention

VTEM's X component data produces crossover type anomalies. This is unlike the Z component of maxima or minima above conductors. During acquisition the convention is for X coil data to be positive in the direction of flight. In the processing phase the polarity is adjusted to follow the right hand rule for multi-component transient electromagnetic methods.

For N-S lines the sign convention for the X in-line component crossover is positive-negative pointing south to north for vertical plate conductors perpendicular to the profile. For E-W lines the sign convention for the X in-line component crossover is positive-negative pointing west to east for vertical plate conductors perpendicular to the profile. X component data for alternating/opposite flight directions are reversed (multiplied by negative one) in the final database to account for this polarity convention.

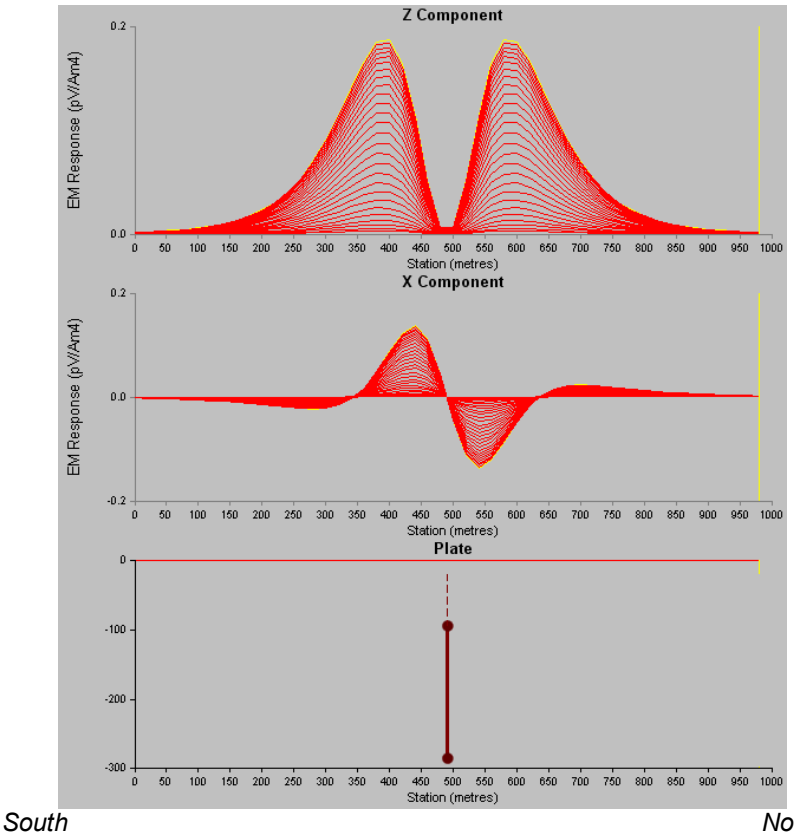

Figure 1: Z- and X-component responses over vertical plate conductor indicating sign convention for X component data.

6.2. *Fraser Filter and Stacked Fraser Filter*

The Fraser Filter converts crossovers of the correct polarity into peak responses of X component by differencing successive values. It is calculated as $(f_1+f_2)-(f_3+f_4)$ where f_i are data from four consecutive stations. This is a derivative filter and likely to increase any noise in data.

A useful presentation of X-component data is the Staked Fraser Filter. The Stacked Fraser Filter data are calculated as the average value of 11 channels (15 to 25) of Fraser Filtered X-component data. The signal to noise ratio is improved and information from 11 channels are combined into one, which allows easier presentation in grid or map format.

6.3. *Effect of loop tilt*

Whenever the X coil is not aligned exactly vertical, it also measures a part of the Z-component response. When the Z-component response is much larger in amplitude than the X-component response it can dominate the measured X-component data. This becomes especially evident when line polarities are reversed; true X-component responses would be coherent from line to line after polarity correction whereas the Z-component becomes alternating negative and positive responses. An example of this is shown in Fig. 2.

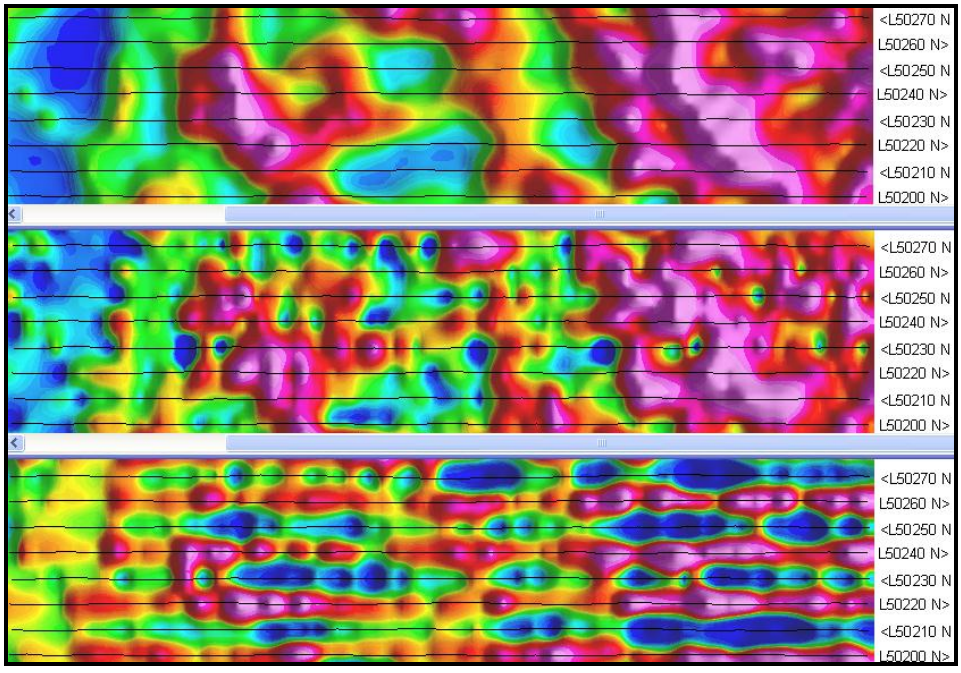

Figure 2: Channel 15 Z-component (top), X-component (middle) and polarity corrected X-component (bottom). The flight line direction is indicated by > or < next to the line number. It is clear that the measured X-component is dominated by Z-component response.

Provided the tilt angle of the coil is known, a correction can be applied to the data. X coil tilt is not measured in with the VTEM system and an approximate procedure was developed to calculate tilt angles in the X-Z plane and remove the Z-component influence on the X-component data.

1.3.1 Quantifying the effect of loop tilt

With Z and X the real vector components and $\underline{Z}$ and $\underline{X}$ the measured components and α the tilt angle of the loop in the line direction, we have:

$$\underline{Z} = Z\cos(\alpha) + X\sin(\alpha)$$
$$\underline{X} = X\cos(\alpha) - Z\sin(\alpha)$$

Over half-space or layered earth environments X=0.

So that:

$$\underline{Z} = Z\cos(\alpha)$$
$$\underline{X} = -Z\sin(\alpha)$$

and

$$\alpha = \text{atan}(-\underline{X}/\underline{Z}).$$

Any value of $\underline{X}$ is therefore ascribed to the term $-Z\sin(\alpha)$. This is sometimes observed in VTEM data with measured X values being negative in general and following inverse trends from the Z-component data (Fig. 3).

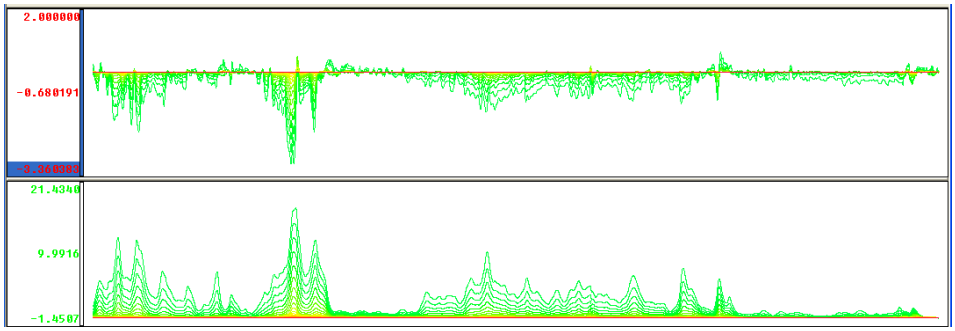

Figure 3: X-component (top) and Z-component (bottom) VTEM data.

1.3.2 *Approximate calculation of loop tilt*

The equation α=atan(-X/ Z) is used to calculate approximate tilt-angles at each position for all channels. An average tilt angle is calculated from channels 15 to 20 and filtered with:

Non-Linear filter: 100 fids; 0.2 sensitivity
LP filter: 500 fids.
(Parameters are determined empirically for individual data sets)

The filtering ensures that anomalous X responses are excluded from subsequent calculations, but also causes small errors in the correction factor. As a final step and average tilt angle (α) for each line is calculated.

1.3.3 *Correcting X-component data*

A new channel for X-component data is calculated as:

SLx_Angle_Corrected= X *cos(α)+Z *sin(α).

The results are to centre responses round zero and visually enhance the occurrences of X-component anomalies (Fig. 4).

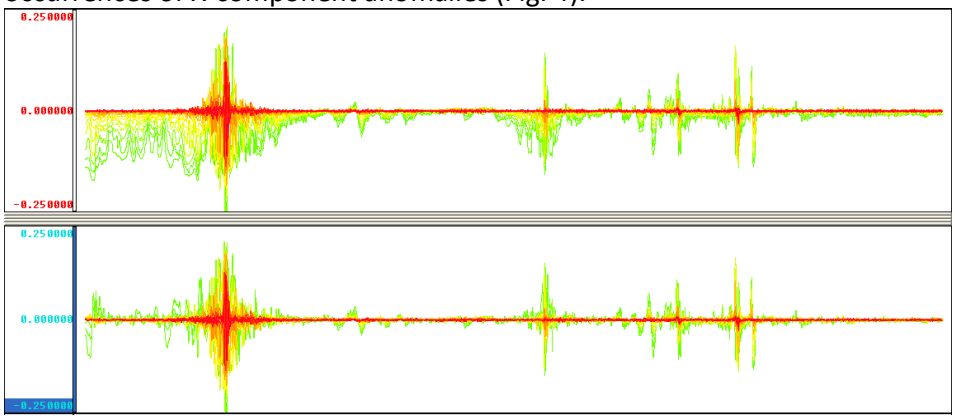

Figure 4: X-component data before (top) and after (bottom) approximate tilt correction.

As this is an approximate correction only, the corrected data might not give accurate results in quantitative modeling or inversions.

The results of the tilt correction and subsequent polarity corrections on gridded data are shown in Fig. 5. After the tilt correction the long wavelength similarities between X- and Z-coil data is no longer evident. The polarity correction now improves line-to-line continuity of as expected.

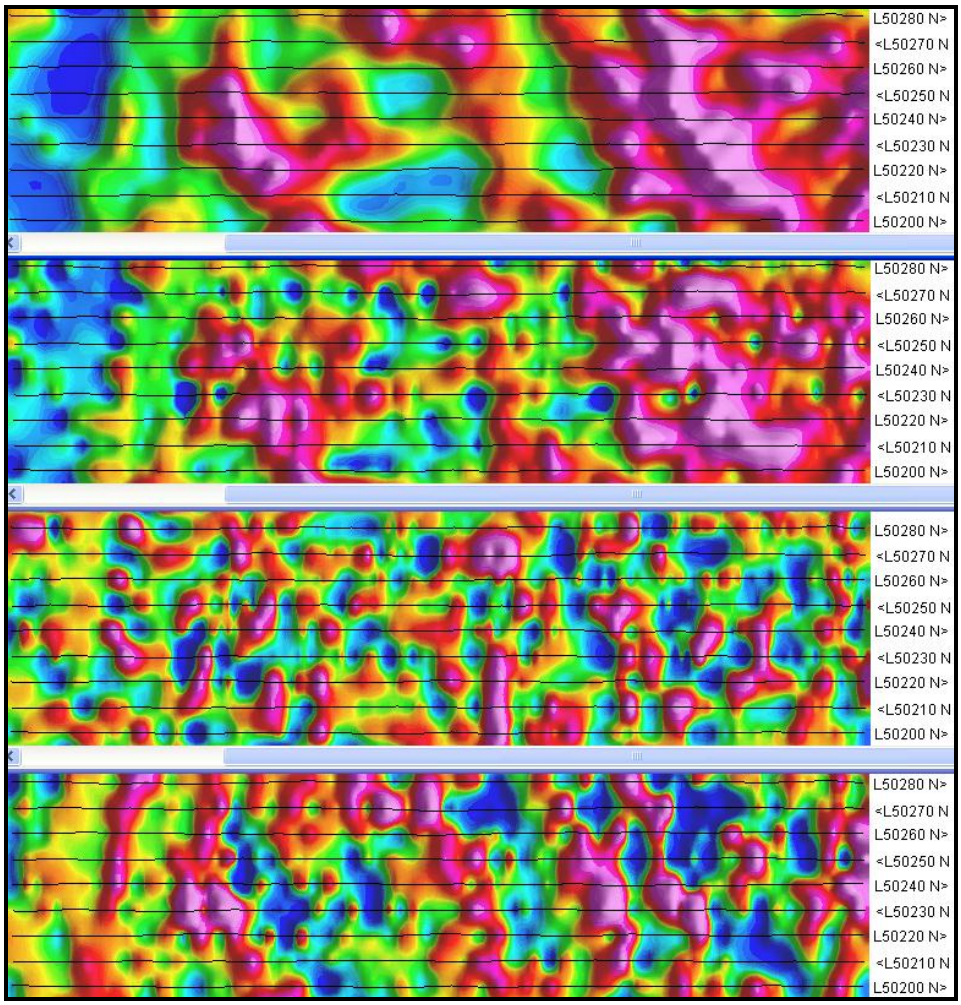

Figure 5: Channel 15 Z-component (top), X-component (second from top), X-component corrected for tilt (second from bottom) and polarity corrected X-component after tilt correction (bottom).

6.4. Typical X-component responses

Forward modeled X- and Z-component responses for some typical plate models in free air are provided below as reference. These were calculated with Maxwell software.

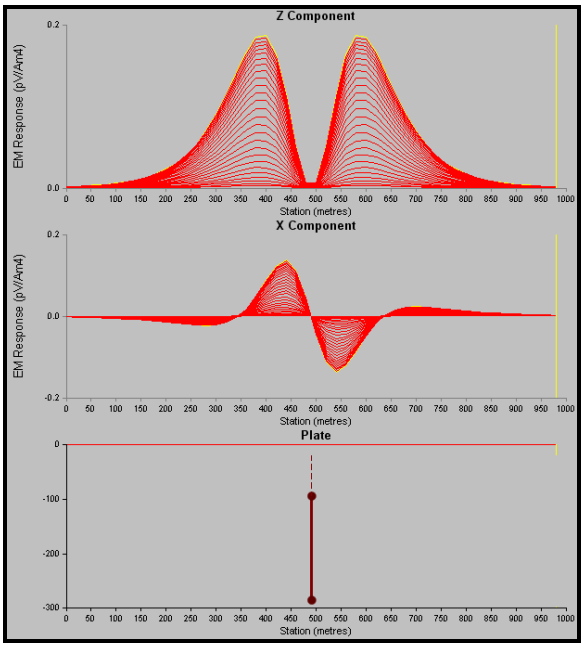

VERTICAL PLATE

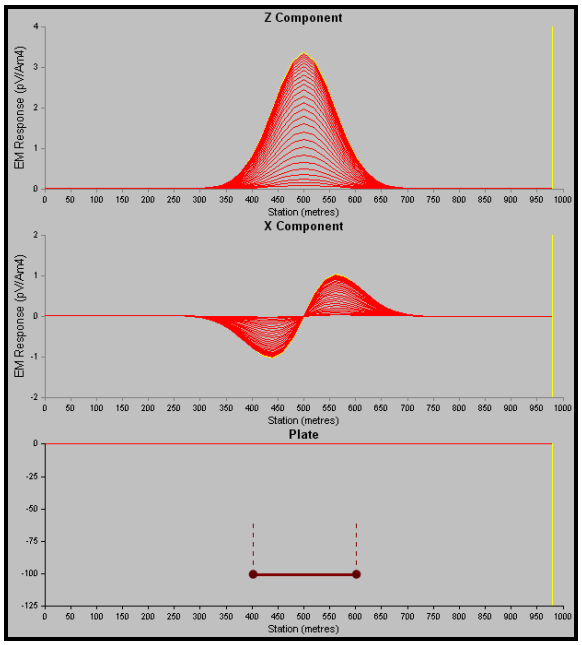

HORIZONTAL PLATE

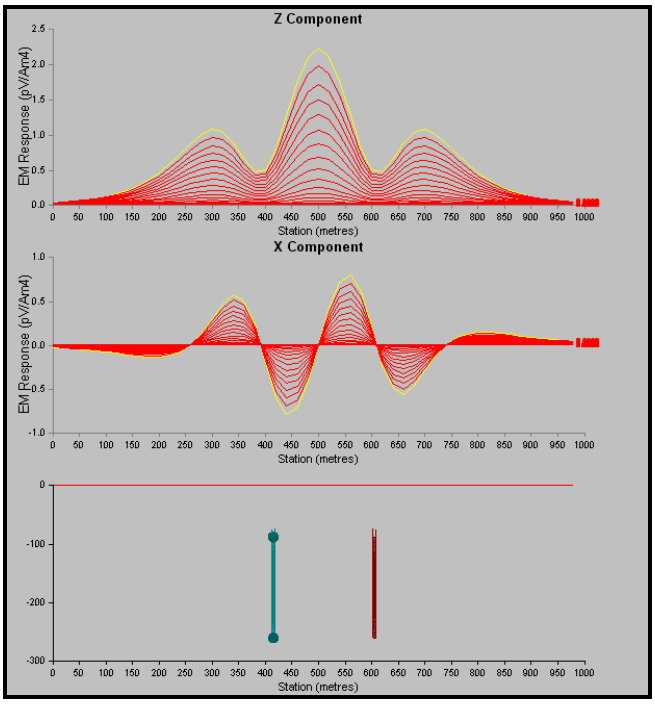

TWO VERTICAL PLATES 200m APART

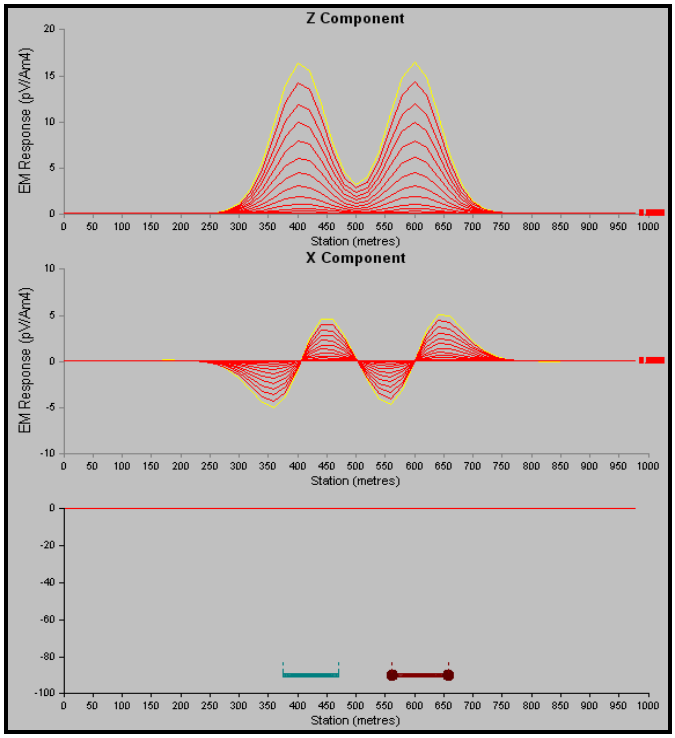

TWO HORIZONTAL PLATES; EDGES 100m APART

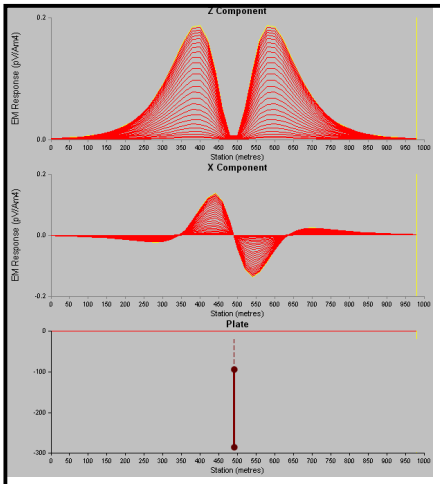

90 degrees

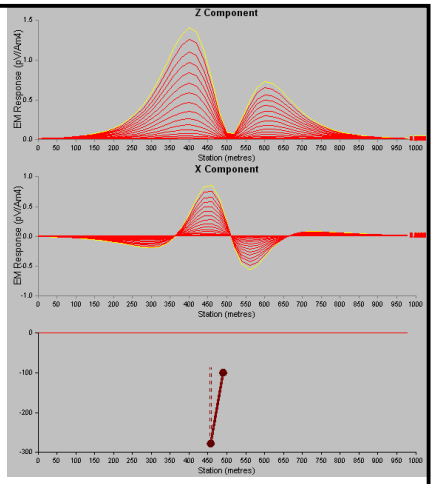

80 degrees

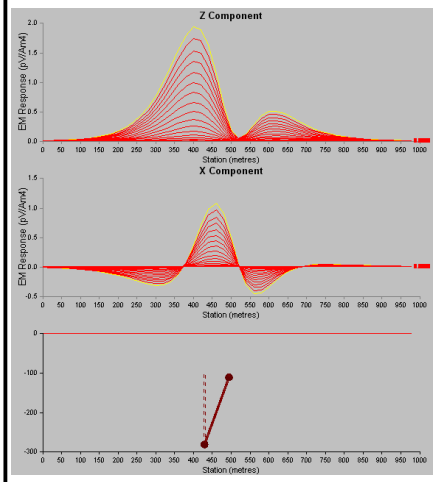

70 degrees

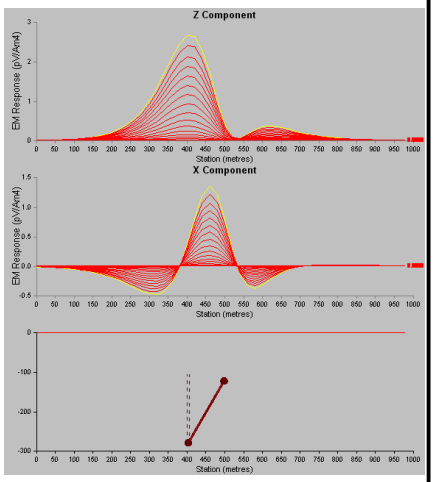

60 degrees

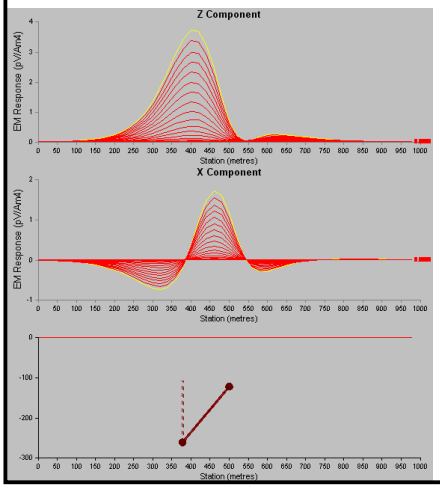

50 degrees

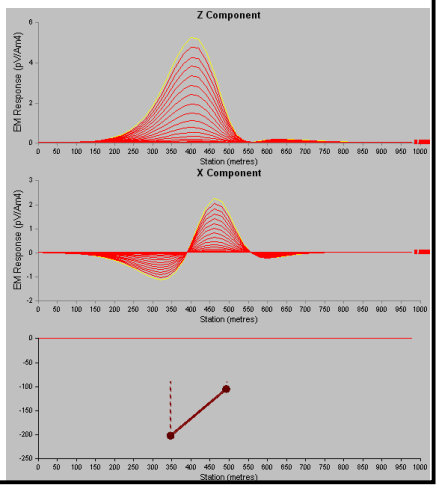

40 degrees

VARIATION WITH DIP

APPENDIX C

GEOPHYSICAL MAP IMAGES
(not to scale)

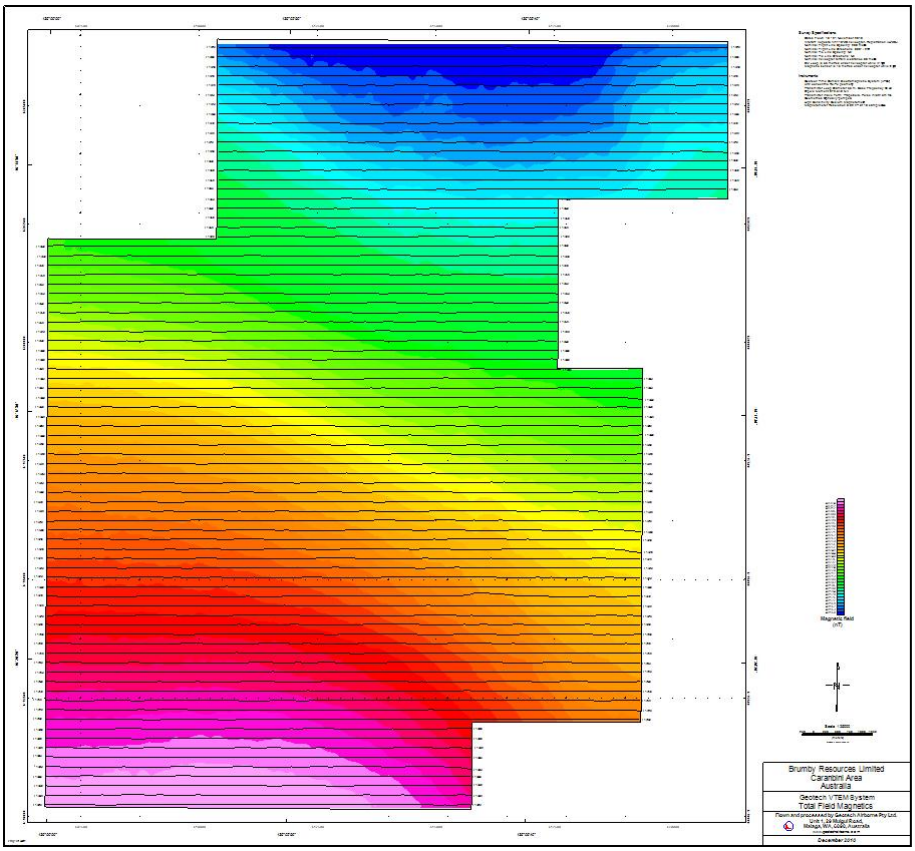
Brumby Resources Limited
Carambin Area
Australia
Geotech VTEM System
Total Field Magnetics
December 2010

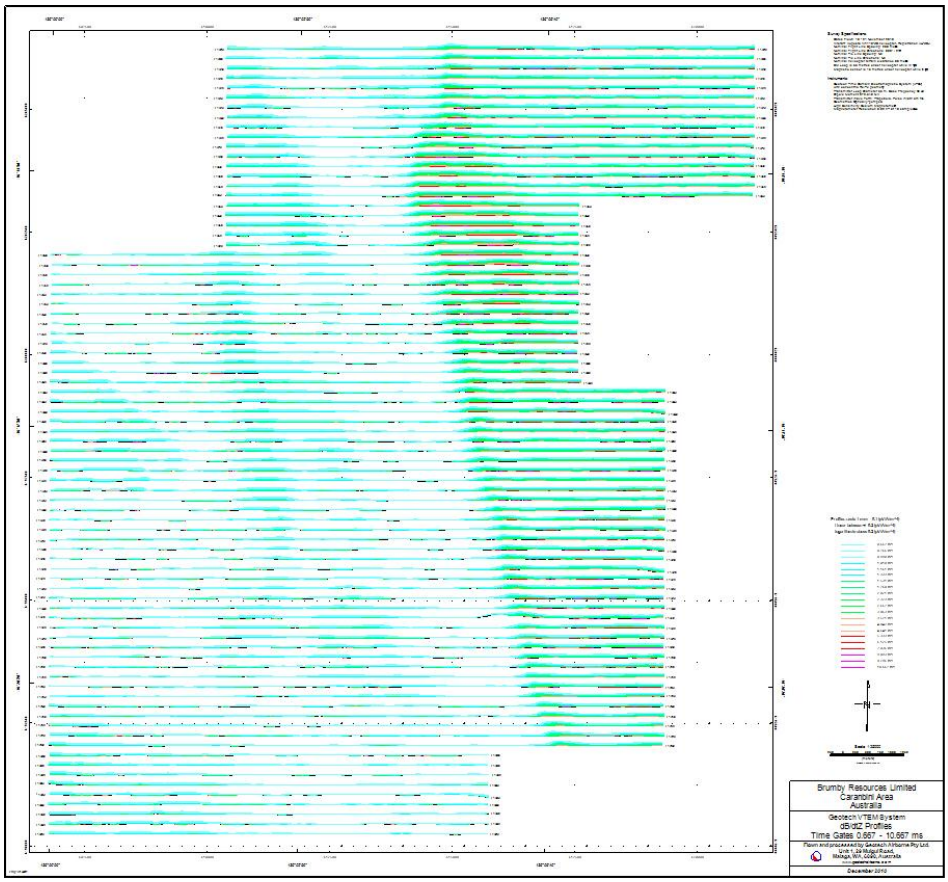
Brumby Resources Limited
Carandini Area
Australia
Geotech VTEM Bi-System
dB/dt Z Profiles
Time Gates 0.667 - 10.667 ms
December 2012

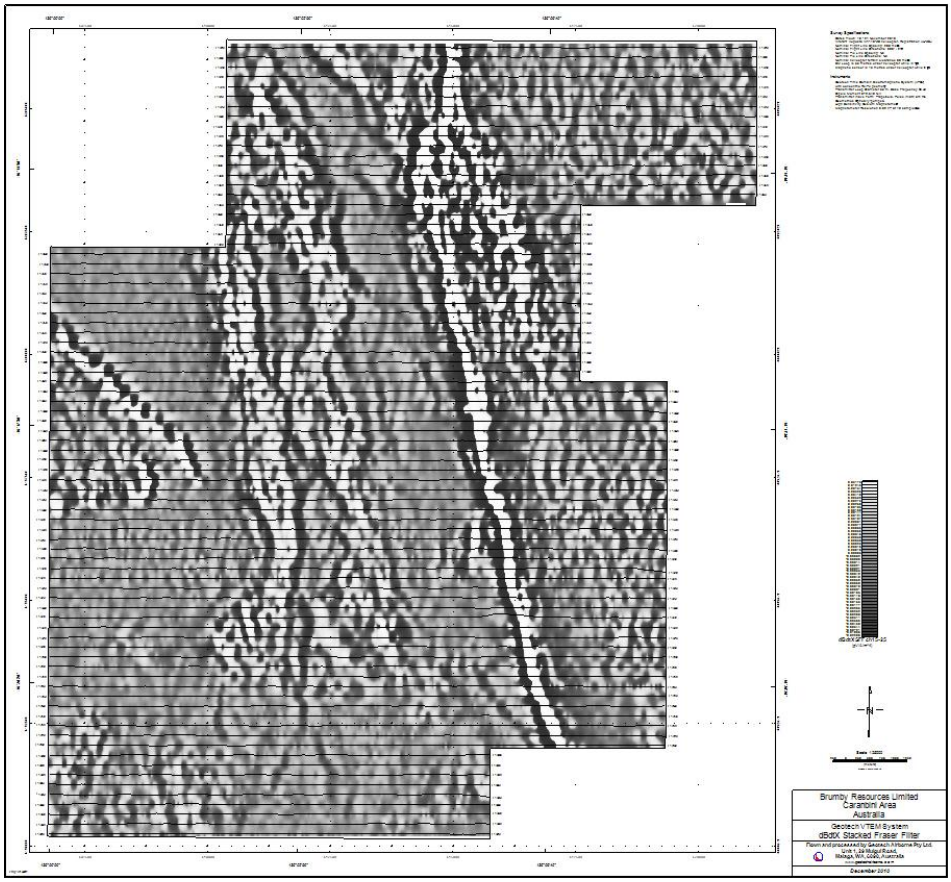
Brumby Resources Limited
Garanbin Area
Australia
Geotech VTEM System
dBdtX Stacked Fraser Filter
December 2012

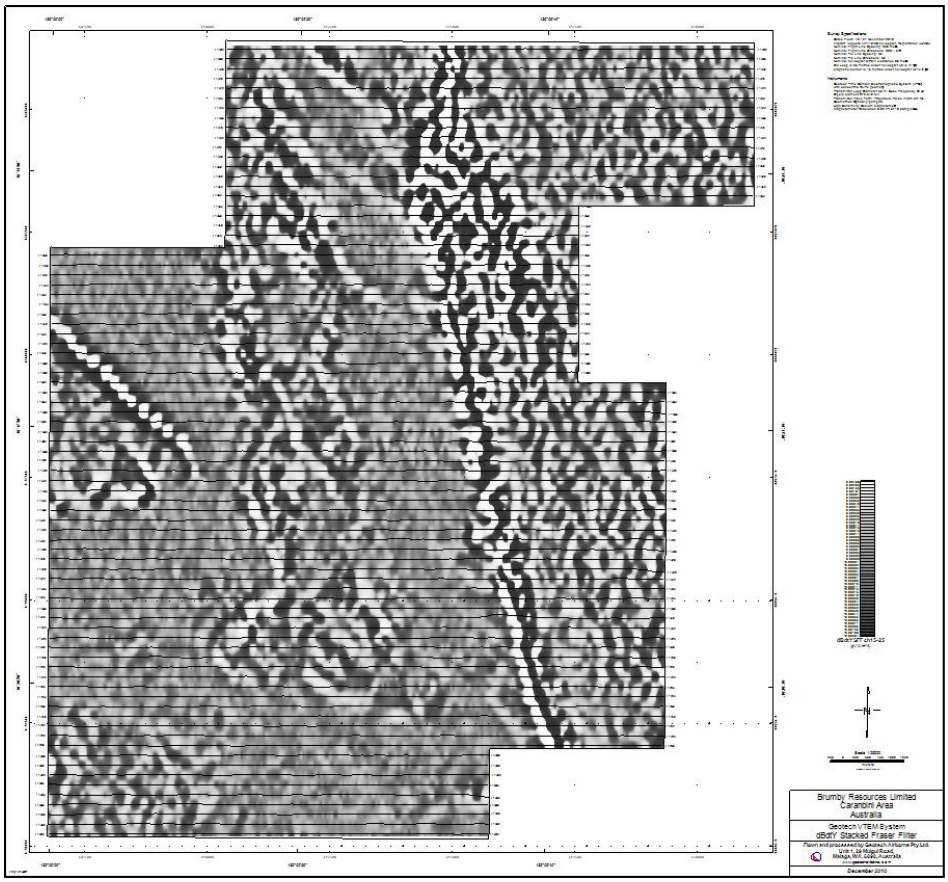
Brumby Resources Limited
Carambin Area
Australia
Geotech VTEM System
dBdT Stacked Fraser Filter
December 2012

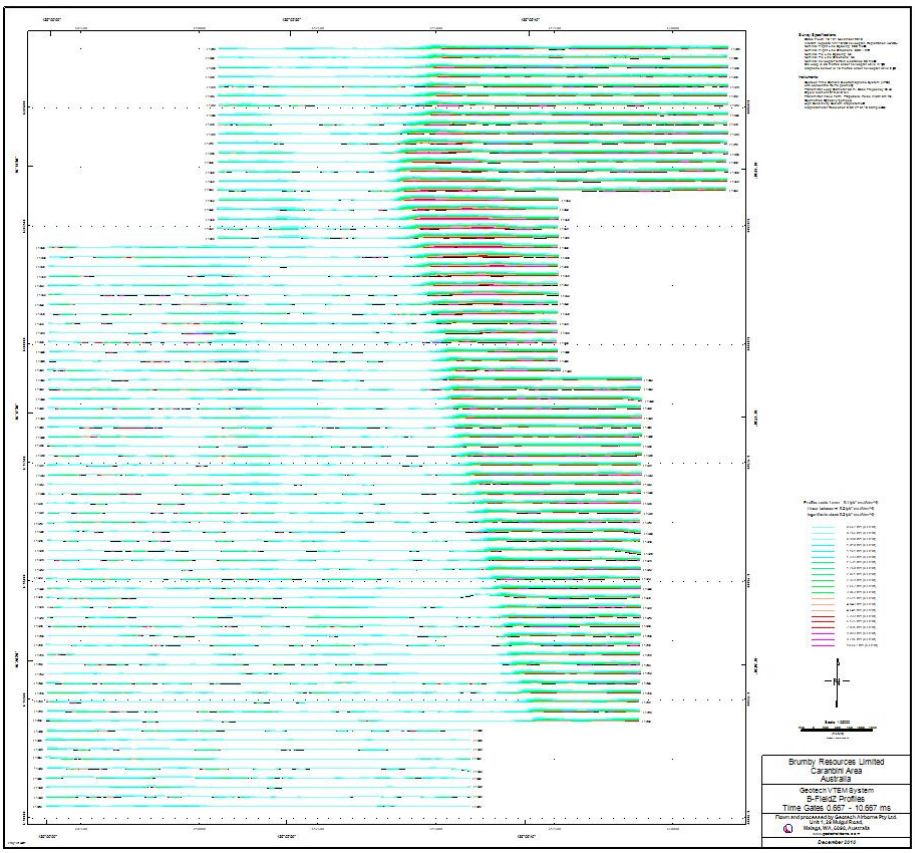
Brumby Resources Limited
Caramomi Area
Australia
Geotech VTEM System
B-Field Z Profiles
Time Gates 0.667 - 10.667 ms
December 2012

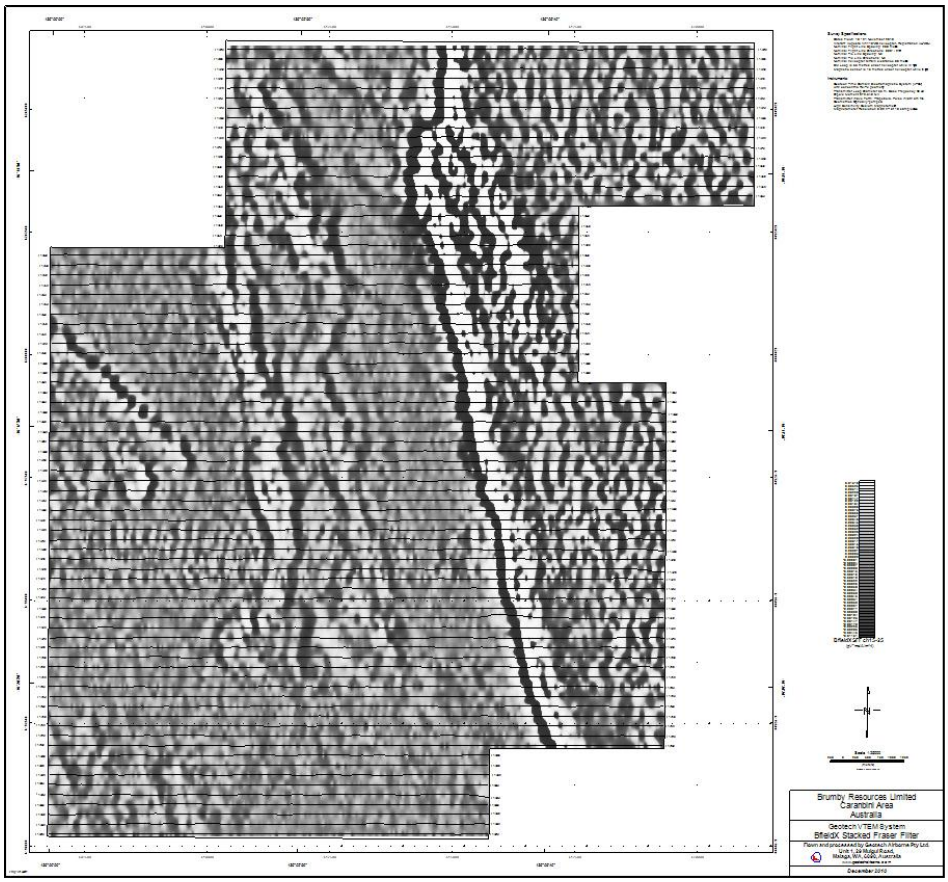
Brumby Resources Limited
Carambin Area
Australia
Geotech VTEM System
Bfield Stacked Fraser Filter
December 2012

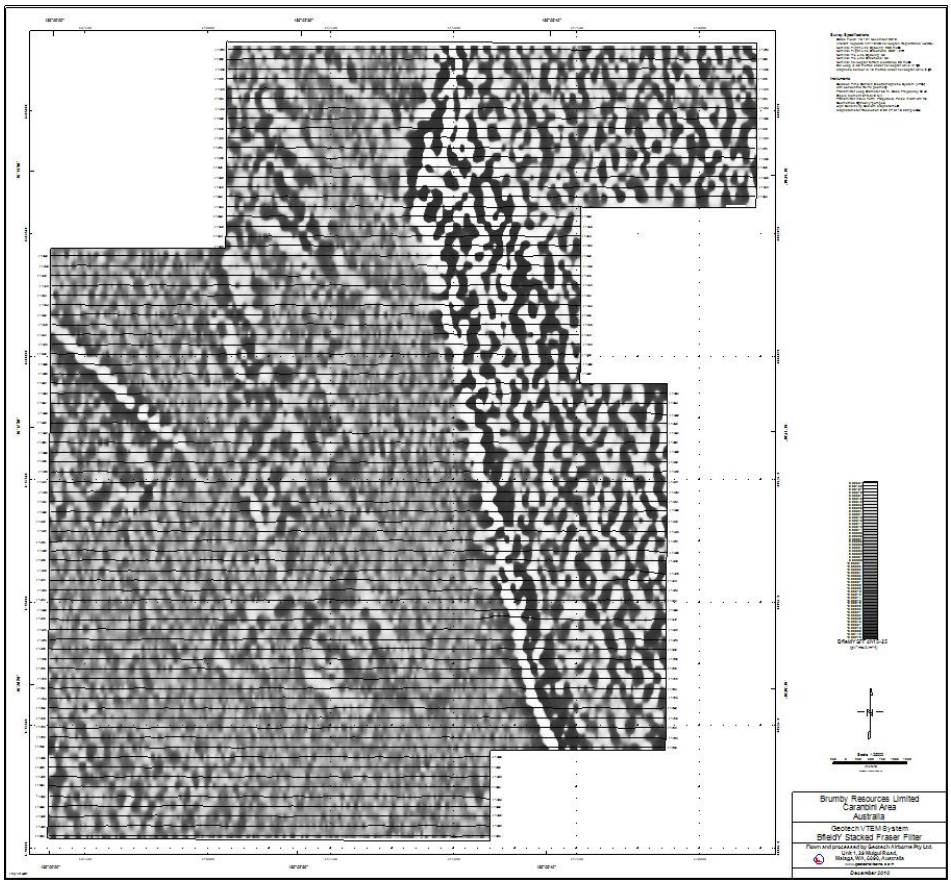
Brumby Resources Limited
Caranbirini Area
Australia
Geotech VTEM System
Steidy Stacked Fraser Filter
December 2012